IOP PUBLISHING JOURNAL OF PHYSICS D: APPLIED PHYSICS

J. Phys. D: Appl. Phys. **42** (2009) 194001 (19pp) doi:10.1088/0022-3727/42/19/194001

REVIEW ARTICLE

Recent advances in the application of Boltzmann equation and fluid equation methods to charged particle transport in non-equilibrium plasmas

R D White[1], R E Robson[1,2], S Dujko[1,3], P Nicoletopoulos[4] and B Li[5]

[1] ARC Centre for Antimatter-Matter Studies, School of Engineering and Physical Sciences, James Cook University, Townsville 4810, Australia
[2] ARC Centre for Antimatter-Matter Studies, Research School of Physical Sciences, Australian National University, Canberra 2600, Australia
[3] Institute of Physics, University of Belgrade, PO Box 68, 11080 Zemun, Belgrade, Serbia
[4] Faculté des Sciences, Université Libre de Bruxelles, 1050 Brussels, Belgium
[5] School of Physics, University of Sydney, Sydney 2006, Australia

E-mail: Ronald.White@jcu.edu.au

Received 7 April 2009, in final form 12 June 2009
Published 18 September 2009
Online at stacks.iop.org/JPhysD/42/194001

Abstract
The kinetic theory of charged particles in gases has come a long way in the last 60 years or so, but many of the advances have yet to find their way into contemporary studies of low-temperature plasmas. This review explores the way in which this gap might be bridged, and focuses in particular on the analytic framework and numerical techniques for the solution of Boltzmann's equation for both electrons and ions, as well as on the development of fluid models and semi-empirical formulae. Both hydrodynamic and non-hydrodynamic regimes are considered and transport properties are calculated in various configurations of dc and ac electric and magnetic fields. We discuss in particular the duality in transport coefficients arising from non-conservative collisions (attachment, ionization).

(Some figures in this article are in colour only in the electronic version)

1. Introduction

The investment of resources internationally in technologies associated with low-temperature plasmas is substantial, with the contribution to the world economy amounting to many billions of dollars. Given the ever increasing need for greater precision, the full potential of this technology can be realized only when the basic physics has been mastered [1, 2]. Moreover there is also a need to understand more fully such diverse scientific and technological applications as astrophysics, lasers, atmospheric physics and high energy particle detectors. What is required in all such cases is first and foremost a theoretical framework capable of dealing with highly non-equilibrium situations, and the kinetic theory of gases, based upon the famous equation developed by Boltzmann in 1872 [3], is ideal for this purpose. PIC codes, Monte Carlo simulation techniques and hybrid methods [4–6] offer complementary and sometimes more advantageous alternatives, but for the present we deal exclusively with kinetic theory. Our paper differs in style and substance from others in the modern plasma literature (see, e.g. [7]) in two important respects, in that we explore the links with (i) the literature on swarms (the test particle limit of a plasma), particularly in regard to solution techniques for the Boltzmann equation and development of fluid models and (ii) the atomic and molecular physics community, who after all provide the cross sections

(measured in the laboratory or calculated theoretically) for input into the Boltzmann equation or fluid models. Indeed there is a strong connection between these two fields, since swarm experiments have traditionally provided the most accurate information about both ion–atom and ion–molecule interaction potentials and low energy (<1 eV) electron impact cross sections [8–11]. It is important to note that experimental swarm transport coefficient data can be 'unfolded' to yield these cross sections only in combination with an accurate kinetic theory. This same kinetic theory can then be used to understand low-temperature plasmas: in the former, one goes from the macroscopic to the microscopic picture, and vice versa for the latter case. This theme will be developed further in this paper. A brief review of the modern kinetic theory literature will serve to put the field in better perspective.

In the 1950s there were a number of seminal papers in the kinetic theory of charged particles in gases, notably by Wannier [12], Allis [13] and Waldmann [14], but it was not until some time later that the modern era can truly be said to have begun. Firstly, Kumar [15–17] introduced the ideas of atomic and nuclear physics into kinetic theory, in particular the techniques of irreducible spherical tensor analysis and separation of centre-of-mass and relative velocity coordinates through the Talmi transformation. Secondly, Viehland, Mason and collaborators formulated the first strong field solution of Boltzmann's equation for ions [18, 19], which in turn laid the basis for the first general solution of Boltzmann's equations for electrons [20]. This connection between ion and electron kinetic theory is something we emphasize in this paper. These developments were summarized in a review in 1980 by Kumar *et al* [21] and have since been discussed in a number of books [8, 22, 23] and reviews [24–26].

One thing we emphasize at the outset is that while these days there are far more applications to low-temperature plasmas than to experiments associated with *swarms* (free diffusion limit of a plasma), there is nevertheless a considerable overlap from a pure kinetic theory perspective. In addition, there are many significant applications outside traditional gaseous electronics, e.g. multi-wire drift tube detectors in high energy particle detectors, muon catalysed fusion, Franck–Hertz oscillations and so on. The points that we think are particularly important are as follows:

- It is neither necessary nor desirable to arbitrarily divide kinetic theory according to the mass of the particles under consideration—electrons and ions may be treated on an equal footing, starting from the *same point*, namely the Boltzmann equation [3] and its semi-classical generalization by Wang-Chang *et al* [27].
- These kinetic equations in phase space may now be solved for the phase space distribution function $f(\boldsymbol{r}, \boldsymbol{c}, t)$ to high accuracy without relying on any of the traditional approximations, e.g. assumptions of near-isotropy in velocity space for light particles.
- Non-conservative collisions (e.g. ionization electron attachment, ionization, ion–molecule collisions) are now recognized to produce *two* fundamentally different families of transport coefficients.
- Fluid models of plasmas are best thought of as a projection of Boltzmann's equation in phase space onto a set of equivalent though approximate equations in configuration space, with any closure *Ansatz* properly benchmarked against exact results whenever possible.

Further discussion of these points, together with examples follows in sections 2–4.

Before embarking on this task, we reiterate that other techniques, such as Monte Carlo, PIC and hybrid modelling, are often favoured for plasmas, because of their complexity, and because of the difficulty in applying boundary conditions to solutions of Boltzmann's equation. These, like kinetic equation treatments, should, however, be benchmarked and their results should reduce to the swarm results in the free diffusion limit. Considerable effort has been invested recently by various groups in benchmarking Boltzmann equation and Monte Carlo simulation codes for electron (and ion) swarms in a variety of electric and magnetic field configurations and forms to understand complex kinetic phenomena present in low-temperature r.f and magnetized plasmas (Belgrade group see e.g. [10, 28–31], JCU group see, e.g. [24, 25, 32–36], Greifswald group see, e.g. [37–39] and others [40–42]). The importance of swarms to low-temperature plasmas has been emphasized in a number of recent papers [10, 11, 24, 25, 30] and also the companion paper by Petrović *et al* in this issue and we refer the reader to these papers for further discussion.

We begin this paper with an overview of the formalism associated with a kinetic treatment of low-temperature plasmas. We then discuss the general solution of the Boltzmann equation including a unified procedure for treating electrons and ions within these plasmas. Both the hydrodynamic and non-hydrodynamic solution regimes are considered and detailed, including a prescription for the calculation of transport coefficients when non-conservative processes such as ionization and attachment are present. This is followed by a fluid equation description of low-temperature plasmas in both the hydrodynamic and non-hydrodynamic regimes, highlighting (i) the utility of momentum transfer theory for evaluating collisional terms in the balance equations and (ii) closure assumptions and approximations. Finally, we conclude with results from cases of special interest, highlighting recent new results, the generality of the theory and associated Boltzmann and fluid codes, and accuracy of fluid equation treatments and other approximations commonly used.

2. Plasma kinetic theory

2.1. Formalism and the Boltzmann equation

The general problem of plasma kinetic theory is summarized in figure 1. By definition [2, 25] a plasma comprises both positive and negative charges, i.e. ions and electrons, and a full kinetic treatment of a plasma therefore requires solution of a kinetic equation for each charged species. In the very low density 'test particle' or 'swarm' limit, such coupling is negligible, and one can solve the ion and electron kinetic equations separately, accounting for collisions with neutral

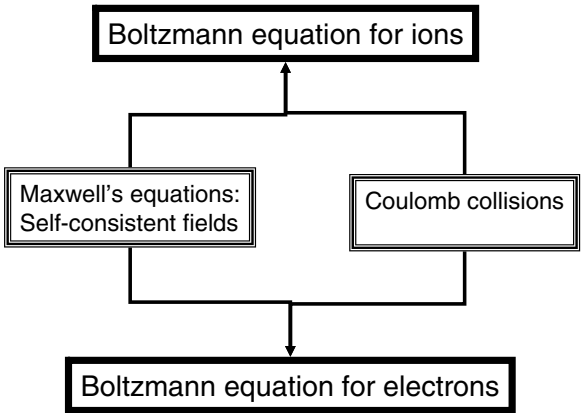

Figure 1. Schematic diagram showing the coupling between Boltzmann kinetic equations for ions and electrons comprising a plasma.

atoms and molecules only. If densities are high enough for space-charge effects to become important (but not charge–charge Coulomb interactions) then Maxwell's equations come into play, but otherwise the kinetic equations we have to solve are the *same* as for the swarm limit. This means that many of the techniques and formalism developed in the past for ion and electron swarms can be brought to bear on the plasma problem, a fact which is still not generally recognized by the plasma community. Of even greater concern is that ion kinetic theory, i.e. one half of the plasma problem, is often neglected. This is in spite of the fact that techniques for solution of Boltzmann's equation for ion in gases have been developed to levels of sophistication comparable to or even exceeding those for electrons [43] over a long period of time (see [22] for a review). In earlier days plasma researchers recognized the need to consider ions and electrons simultaneously—see, for example, the seminal paper of Allis [13]—but in the meantime there has been a divergence of the respective literatures. Real progress in plasma kinetic theory depends upon this connection being re-established.

We now quantify the elements of figure 1. The Boltzmann kinetic equation for each charged component i of a weakly ionized gas under the influence of electric $\boldsymbol{E}$ and magnetic $\boldsymbol{B}$ fields can be written as

$$\left[\frac{\partial}{\partial t} + \boldsymbol{c}\cdot\frac{\partial}{\partial \boldsymbol{r}} + \frac{q_i}{m_i}\left[\boldsymbol{E} + \boldsymbol{c}\times\boldsymbol{B}\right]\cdot\frac{\partial}{\partial \boldsymbol{c}}\right] f_i = -J(f_i, F_0) - \sum_{i'} J(f_i, f_{i'}), \tag{1}$$

where $f_i(\boldsymbol{r}, \boldsymbol{c}, t)$ is the phase space distribution function at the position $\boldsymbol{r}$ and velocity $\boldsymbol{c}$, while q_i and m_i are the charge and mass of species i respectively. Also, $J(f_i, F_0)$ and $J(f_i, f_{i'})$ denote the collision terms for charged particle–neutral molecule collisions and charged particle–charged particle interactions, respectively, and F_0 is the neutral velocity distribution. Put in a nutshell, the problem of kinetic theory is to solve the set of equations (1) for $f_i(\boldsymbol{r}, \boldsymbol{c}, t)$ with appropriate boundary and initial conditions and coupled with Maxwell's equation. This is generally a formidable task.

The terms $J(f_i, f_{i'})$ describe interaction between charged particles via the Coulomb force, as represented by the Fokker–Planck operator in velocity space, and symbolically by the right-hand link in figure 1. As explained in text books (see, e.g. [44]) these operators are derivable directly from the usual Boltzmann elastic collision operator, together with a suitable *ad hoc* 'cut-off' procedure for certain divergent integrals. These operators are non-linear in f, making for difficult solutions (see, e.g. [45, 46]).

In the rest of this paper we shall deal with cases where densities are sufficiently low [47] so that such charge–charge interactions are negligible (right-hand link in figure 1 removed) and equation (1) simplifies to

$$\left[\frac{\partial}{\partial t} + \boldsymbol{c}\cdot\frac{\partial}{\partial \boldsymbol{r}} + \frac{q_i}{m_i}\left[\boldsymbol{E}(\boldsymbol{r}, t) + \boldsymbol{c}\times\boldsymbol{B}(\boldsymbol{r}, t)\right]\cdot\frac{\partial}{\partial \boldsymbol{c}}\right] f_i = -J(f_i, F_0). \tag{2}$$

This is of the same form for both plasmas and swarms. However, for plasmas, the fields are calculated self-consistently with Maxwell's equations (left-hand link in figure 1), e.g. Poisson's equation:

$$\nabla\cdot\boldsymbol{E} = \frac{1}{\epsilon_0}\sum_i n_i(\boldsymbol{r}, t) q_i, \tag{3}$$

while for swarms the fields are completely externally prescribed (left-hand link in figure 1 removed).

After solving (2), quantities of physical interest are obtained as velocity 'moments' of the distribution functions, starting with the number density,

$$n_i(\boldsymbol{r}, t) = \int f_i(\boldsymbol{r}, \boldsymbol{c}, t)\,\mathrm{d}\boldsymbol{c} \tag{4}$$

followed by higher order quantities,

$$\langle\phi(\boldsymbol{c})\rangle_i = \frac{1}{n_i(\boldsymbol{r}, t)}\int \phi(\boldsymbol{c}) f_i(\boldsymbol{r}, \boldsymbol{c}, t)\,\mathrm{d}\boldsymbol{c} \tag{5}$$

with $\phi(\boldsymbol{c}) = m\boldsymbol{c}, \frac{1}{2}mc^2, \ldots$ furnishing the average velocity $\boldsymbol{v}_i$, average energy ϵ_i, and so on.

In what follows, it is possible to suppress the charged particle species index i without any ambiguity arising. Quantities pertaining to the neutral gas will, however, still be delineated by the subscript '0'.

2.1.1. Boundary conditions. Equation (2) can be solved together with boundary and initial conditions on $f(\boldsymbol{r}, \boldsymbol{c}, t)$, appropriate to the physical circumstances. Theorems concerning uniqueness, which have been developed in the context of neutron transport (see, e.g. [48]), carry over to the present problem. One has to be careful not to over-specify $f(\boldsymbol{r}, \boldsymbol{c}, t)$ on the bounding surface Σ: thus only the value of the distribution function for velocities pointing *into* the volume bounded by this surface should be specified, i.e. if $\boldsymbol{\sigma}$ is a unit vector normal to Σ, pointing inwards, we can specify only

$$f(\boldsymbol{r}, \boldsymbol{c}, t), \qquad \boldsymbol{c}\cdot\boldsymbol{\sigma} > 0 \tag{6}$$

on Σ. It is very difficult to solve (2) with exact boundary conditions such as this in phase space and typically one resorts to either approximations involving certain moments (5) of $f(\boldsymbol{r}, \boldsymbol{c}, t)$ (see, e.g. [22]) or, in the case of truncated spherical harmonic representations of $f(\boldsymbol{r}, \boldsymbol{c}, t)$ (see equation (31) below), to the Mark conditions [49, 50] in which the expansion coefficients are specified for either even or odd values of l.

The situation is, however, much simpler in the *hydrodynamic regime* (see below), for then all the space-dependence of the distribution function is projected onto the number density $n(\boldsymbol{r}, t)$, symbolically

$$f(\boldsymbol{r}, \boldsymbol{c}, t) = \mathscr{F}(\boldsymbol{c}|n(\boldsymbol{r}, t)), \tag{7}$$

where the right-hand side denotes a linear functional of $n(\boldsymbol{r}, t)$, e.g. the familiar density gradient expansion (see equation (17)). In that case boundary conditions need to be specified only in configuration space, i.e. only on $n(\boldsymbol{r}, t)$, which is in turn found from solution of the diffusion equation (see equation (27)).

For *non-hydrodynamic* situations, however, no such simplification is possible, and the kinetic equation (2) must then be solved with boundary conditions in phase space, approximate or otherwise. This can be the case even in simple geometries, for example a plane surface or source in contact with an otherwise unbounded gas [51–53]. The Franck–Hertz experiment is an example of such a non-hydrodynamic problem [54, 55].

2.1.2. The Boltzmann equation collision term. Collisions between charged particles and neutral gas molecules are described by the right-hand side of (2), which in turn has contributions from a number of processes:

$$J(f, F_0) = J_{\mathrm{WUB}}(f, F_0) + J_R(f, F_0) + J_I(f, F_0) + \cdots, \tag{8}$$

where the Wang-Chang, Uhlenbeck, de Boer semi-classical collision operator describing elastic, inelastic and super elastic collisions is given by [27]

$$J_{\mathrm{WUB}}(f, F_0) = \sum_{jk} \int \left[f(\boldsymbol{r}, \boldsymbol{c}, t) F_{0j}(\boldsymbol{c}_0) - f(\boldsymbol{r}, \boldsymbol{c}', t) F_{0k}(\boldsymbol{c}_0{}') \right] \times g \sigma(jk; g\chi) \, \mathrm{d}\hat{\boldsymbol{g}}' \, \mathrm{d}\boldsymbol{c}_0 \tag{9}$$

and $\sigma(jk; g\chi)$ is the differential cross section for the scattering process $(j, \boldsymbol{c}, \boldsymbol{c}_0) \rightarrow (k, \boldsymbol{c}', \boldsymbol{c}_0')$ where $\cos\chi = \boldsymbol{g} \cdot \boldsymbol{g}'$. If the gas remains in undisturbed equilibrium, then $F_{0j}(\boldsymbol{c}_0)$ is a Maxwell–Boltzmann distribution for neutrals with internal state j. In that case the operator (2) is linear in f. Note that for light particles, (9) can be approximated by the familiar quasi-Lorentz differential form for elastic collisions and the Frost–Phelps finite difference expression for inelastic collisions [21], if so desired. This, however, is not necessary, and it is purely a matter of convenience as to whether one uses the full or approximated expressions.

On the other hand electron attachment and ion–molecule reactions are described by operators of the form

$$J_R(f, F_0) = \sum_j f(\boldsymbol{r}, \boldsymbol{c}, t) \int F_{0j}(\boldsymbol{c}_0) g \sigma_R(j; g) \, \mathrm{d}\boldsymbol{c}_0, \tag{10}$$

where $\sigma_R(j, g)$ is the appropriate 'reactive' cross section. Ionization is a three body problem for which the corresponding operator is [56]

$$J_I(f, F_0) = \sum_j n_{oj} \left\{ c \sigma_I(j; c) f(\boldsymbol{r}, \boldsymbol{c}, t) - 2 \int c' \sigma_I(j; c') B(\boldsymbol{c}, \boldsymbol{c}'; j) f(\boldsymbol{r}, \boldsymbol{c}', t) \, \mathrm{d}\boldsymbol{c}' \right\}, \tag{11}$$

where $\sigma_I(j, c)$ is the ionization cross section and $B(\boldsymbol{c}, \boldsymbol{c}'; j)$ is the probability of one of the two electrons after ionization having a velocity in the range of $\boldsymbol{c}$ to $\boldsymbol{c}+ \mathrm{d}\boldsymbol{c}$, for incident electron velocity $\boldsymbol{c}'$. Normalization requires $\int B(\boldsymbol{c}, \boldsymbol{c}'; j) \, \mathrm{d}\boldsymbol{c} = 1$.

2.2. Solutions regimes—hydrodynamic and non-hydrodynamic

For weak fields and spatial gradients, with a slow time variation and otherwise near-equilibrium conditions, the entire left-hand side of equation (2) is small, and the Chapman–Enskog perturbation solution technique [57, 58] can be applied. To formally illustrate the method, we introduce a small parameter δ and write

$$\delta \left[\frac{\partial f}{\partial t} + \boldsymbol{c} \cdot \frac{\partial f}{\partial \boldsymbol{r}} + \frac{q}{m} [\boldsymbol{E} + \boldsymbol{c} \times \boldsymbol{B}] \cdot \frac{\partial f}{\partial \boldsymbol{c}} \right] = -J(f, F_0). \tag{12}$$

One then substitutes

$$f = n f^{(0)} + \delta f^{(1)} + \delta^2 f^{(2)} + \cdots \tag{13}$$

equates coefficients of powers of δ, and generates a hierarchy of equations for the $f^{(i)}$. The first member of the hierarchy is

$$J(f^{(0)}, F_0) = 0, \tag{14}$$

which has as its immediate solution that f_0 is a Maxwellian at gas temperature. The higher order members of the hierarchy introduce dependences upon fields and ∇n. Kihara [59] was the first to adapt the Chapman–Enskog method for ions and thus obtained the weak field solution of (2). Given that both low-temperature plasmas and swarms are generally far from equilibrium, this method is not particularly useful for most problems of interest here.

Next suppose that while the space and (implicit) time variation of f are still assumed to be small, the fields and explicit time variation may be strong. Thus we associate the small parameter δ with only the spatial term on the left-hand side of equation (2) and develop an iterative scheme of solution based upon

$$\delta \left[\boldsymbol{c} \cdot \frac{\partial f}{\partial \boldsymbol{r}} \right] + \frac{\partial f}{\partial t} + \frac{q}{m} [\boldsymbol{E} + \boldsymbol{c} \times \boldsymbol{B}] \cdot \frac{\partial f}{\partial \boldsymbol{c}} = -J(f, F_0), \tag{15}$$

together with the expansion (13) again. The first member of the hierarchy is now

$$\frac{\partial f^{(0)}}{\partial t} + \frac{q}{m} [\boldsymbol{E} + \boldsymbol{c} \times \boldsymbol{B}] \cdot \frac{\partial f^{(0)}}{\partial \boldsymbol{c}} = -J(f^{(0)}, F_0), \tag{16}$$

which generally yields an $f^{(0)}$ which deviates significantly from a Maxwellian. The next member of the chain of

equations furnishes $f^{(1)}$ in terms of the density gradient ∇n, the subsequent member $f^{(2)}$ in terms of $\nabla\nabla n$, and so on. Thus equation (13) gives in this case

$$f(\boldsymbol{r},\boldsymbol{c},t) = n(\boldsymbol{r},t)f^{(0)}(\boldsymbol{c},t) + \boldsymbol{f}^{(1)}(\boldsymbol{c},t)\cdot\nabla n + \boldsymbol{f}^{(2)}(\boldsymbol{c},t):\nabla\nabla n + \cdots, \tag{17}$$

the familiar *density gradient expansion* [21] generalized to explicit sources of time dependence, where $f^{(j)}(\boldsymbol{c})$ denotes a tensor of rank j. Clearly the assumption of a hydrodynamic regime is implicit in this procedure, with (17) being a particular example of the general representation (7). The corresponding expansions for the most important physical quantities are found by forming moments of this expression as in (5). Thus we obtain

$$\boldsymbol{\Gamma}(\boldsymbol{r},t) = n\langle\boldsymbol{c}\rangle = \boldsymbol{W}_{\mathrm{F}}(t)n(\boldsymbol{r},t) - \boldsymbol{D}_{\mathrm{F}}(t)\cdot\nabla n(\boldsymbol{r},t) + \cdots, \tag{18}$$

$$S(\boldsymbol{r},t) = \int J_R(f,F_0)\,\mathrm{d}\boldsymbol{c} = S^{(0)}(t)n(\boldsymbol{r},t) + \boldsymbol{S}^{(1)}(t)\cdot\nabla n(\boldsymbol{r},t) + \boldsymbol{S}^{(2)}(t):\nabla\nabla n(\boldsymbol{r},t) + \cdots, \tag{19}$$

$$\epsilon(\boldsymbol{r},t) = \langle\tfrac{1}{2}mc^2\rangle(\boldsymbol{r},t) = \varepsilon(t) + \frac{\boldsymbol{\gamma}(t)}{n}\cdot\nabla n(\boldsymbol{r},t) + \cdots, \tag{20}$$

where

$$\boldsymbol{W}_{\mathrm{F}}(t) = \frac{1}{n}\int \boldsymbol{c}f^{(0)}(\boldsymbol{c},t)\,\mathrm{d}\boldsymbol{c}, \tag{21}$$

$$\boldsymbol{D}_{\mathrm{F}}(t) = -\frac{1}{n}\int \boldsymbol{c}\boldsymbol{f}^{(1)}(\boldsymbol{c},t)\,\mathrm{d}\boldsymbol{c}, \tag{22}$$

$$\boldsymbol{S}^{(i)}(t) = \frac{1}{n}\int J_R(f^{(i)},F_0)\,\mathrm{d}\boldsymbol{c}, \tag{23}$$

$$\varepsilon(t) = \frac{1}{n}\int \tfrac{1}{2}mc^2 f^{(0)}(\boldsymbol{c},t)\,\mathrm{d}\boldsymbol{c}, \tag{24}$$

$$\boldsymbol{\gamma}(t) = \frac{1}{n}\int \tfrac{1}{2}mc^2\boldsymbol{f}^{(1)}(\boldsymbol{c},t)\,\mathrm{d}\boldsymbol{c}. \tag{25}$$

Equations (21)–(25) define the most important hydrodynamic transport coefficients and reaction rates.

In cases where a hydrodynamic description is not possible, then all members of (2) must be treated at the same level. One cannot project out the space–time dependence of the distribution function onto the number density, as in (7), or make an expansion as in (17), and transport coefficients are not meaningful quantities. Instead of solving a hierarchy of equations in three-dimensional velocity space only, one must solve equation (2) with at least one additional configuration space dimension. This makes for a very demanding computational problem.

2.2.1. Transport coefficient duality—the Tagashira–Sakai–Sakamoto (TSS) effect. If we integrate (2) over all velocities there results the equation of continuity,

$$\frac{\partial n(\boldsymbol{r},t)}{\partial t} + \nabla\cdot\boldsymbol{\Gamma}(\boldsymbol{r},t) = S(\boldsymbol{r},t), \tag{26}$$

which is exact, but not particularly useful. If the hydrodynamic regime prevails, we can substitute for particle flux and reaction rate from (18) and (19) respectively, to obtain the diffusion equation

$$\frac{\partial n}{\partial t} + \boldsymbol{W}(t)\cdot\nabla n - \boldsymbol{D}(t):\nabla\nabla n = S^{(0)}(t)n, \tag{27}$$

which defines the bulk drift velocity and diffusion tensor

$$\boldsymbol{W}(t) = \boldsymbol{W}_{\mathrm{F}}(t) - \boldsymbol{S}^{(1)}(t), \tag{28}$$

$$\boldsymbol{D}(t) = \boldsymbol{D}_F(t) - \boldsymbol{S}^{(2)}(t), \tag{29}$$

respectively.

The diffusion equation (27) is generally used to unfold swarm experiments to yield $\boldsymbol{W}(t)$ and $\boldsymbol{D}(t)$, not the flux–gradient relation (18). It is thus the bulk transport coefficients, not the flux quantities, which are tabulated in the swarm literature. Differences are often significant ranging from a few percent to orders of magnitude [24, 56, 60]. In some cases, however, bulk and flux transport coefficients may exhibit completely different qualitative behaviour, as in cases of negative absolute electron flux mobility (but not bulk mobility) for strongly attaching gases [61, 62] and negative differential conductivity (NDC) for positron bulk drift velocity (but not flux drift velocity) [63]. In the absence of reactions, i.e. $S = 0$, the two sets of coefficients coincide. It is clear that care is required to use the correct swarm transport data in fluid models [25]. The duality in transport coefficients is easy to understand physically [64] and the phenomenon is referred to in our work as the Tagashira–Sakai–Sakamoto (TSS) effect, in recognition of those researchers who first made the distinction between the two types of transport quantities [65, 66].

2.3. Space and time dependent multi-term solution of Boltzmann's equation

2.3.1. Velocity space representations. The first step in any analysis is typically the representation of the distribution function in directions of velocity space through an expansion in spherical harmonics $Y_m^{[l]}(\hat{\boldsymbol{c}})$

$$f_i(\boldsymbol{r},\boldsymbol{c},t) = \sum_{l=0}^{\infty}\sum_{m=-l}^{l} f_{i,m}^{(l)}(\boldsymbol{r},c,t)Y_m^{[l]}(\hat{\boldsymbol{c}}), \tag{30}$$

where $\hat{\boldsymbol{c}}$ denotes the angles of $\boldsymbol{c}$. Note that this reduces to an expansion in terms of Legendre polynomials $P_l(\cos\theta)$ only under very special circumstances of sufficiently high symmetry [64]. In any practical calculation the infinite expansion (30) must be truncated to finite size by imposing an upper limit $l_{\max}$ on the l-summation:

$$f_i(\boldsymbol{r},\boldsymbol{c},t) = \sum_{l=0}^{l_{\max}}\sum_{m=-l}^{l} f_{i,m}^{(l)}(\boldsymbol{r},c,t)Y_m^{[l]}(\hat{\boldsymbol{c}}). \tag{31}$$

For *light particles*, such as electrons undergoing predominantly *elastic* collisions, as is the case in atomic gases at low fields, there are good physical grounds for choosing $l_{\max} = 1$, leading to the so-called *two-term approximation* [64, 67]. For *ions* under *all* circumstances, or for light particles in molecular gases undergoing *inelastic* collisions, it has long been established that a *multi-term analysis* is required, in which $l_{\max}$ must

be varied incrementally until some convergence/accuracy criterion is attained [20]. It is not at all unusual to require an $l_{\max} > 5$ to have transport coefficients accurate to better than 1%, even for electrons [56, 67]. Note that one simply increments $l_{\max}$ until (31) (or integrals involving it) converges to within the desired accuracy. There are *no* fundamental reasons for specifying it as either odd or even. The particular *numerical algorithm* used for solution may well require such a restriction, but the equations by themselves do not. These two things should be carefully distinguished.

The next step is to represent the expansion coefficients in (31) in speed (or energy) space, and here there are a number of possibilities [24], e.g. following the spirit of traditional kinetic theory [57], through an expansion in terms of Sonine (generalized Laguerre) polynomials,

$$f_{i,m}^{(l)}(\boldsymbol{r}, c, t) = w(\alpha, c) \sum_{\nu=0}^{\infty} F_i(\nu l m; \alpha, \boldsymbol{r}, t) R_{\nu l}(\alpha c), \quad (32)$$

where the Maxwellian weight function is defined by

$$w(\alpha, c) = \left(\frac{\alpha^2}{2\pi}\right)^{3/2} \exp\left\{\frac{-\alpha^2 c^2}{2}\right\} \quad (33)$$

and $\alpha^2 = m/kT_{\mathrm{b}}$. The modified Sonine polynomials satisfy the orthonormality relation

$$\int_0^{\infty} w(\alpha, c) R_{\nu' l}(\alpha c) R_{\nu l}(\alpha c) c^2 \, \mathrm{d}c = \delta_{\nu' \nu}. \quad (34)$$

In the modern approach one sets T_{b} to be the ion temperature [22] or an arbitrary basis temperature [20]. Putting (31) and (32) together gives

$$f_i(\boldsymbol{r}, \boldsymbol{c}, t) = w(\alpha, c) \sum_{\nu=0}^{\infty} \sum_{l=0}^{\infty} \sum_{m=-l}^{l} F_i(\nu l m; \alpha, \boldsymbol{r}, t) \phi_m^{[\nu l]}(\boldsymbol{c}), \quad (35)$$

where $\phi_m^{[\nu l]}(\boldsymbol{c}) = R_{\nu l}(\alpha c) Y_m^{[l]}(\hat{\boldsymbol{c}})$ is a Burnett function [15].

2.3.2. Matrix representation of the full space–time Boltzmann equation. After substituting (35) into (2), we eventually obtain the following infinite set of partial differential equations for the moments $F_i(\nu l m; \alpha, \boldsymbol{r}, t)$ corresponding to species i:

$$\sum_{\nu'=0}^{\infty} \sum_{l'=0}^{\infty} \sum_{m'=-l'}^{l'} \left[\left(\frac{\partial}{\partial t} + (J_i)_{\nu\nu'}^{l} \right) \delta_{l'l} \delta_{m'm} + \left\langle \nu l m || \boldsymbol{c} \cdot \nabla + \boldsymbol{a} \cdot \frac{\partial}{\partial \boldsymbol{c}} || \nu' l' m' \right\rangle + \sum_{\nu''=0}^{\infty} \sum_{l''=0}^{\infty} \sum_{m''=-l''}^{l''} (l' m' l'' m'' | l m) \sum_{i'} (J_{i,i'})_{\nu\nu'\nu''}^{l l' l''} F_{i'}'(\nu'' l'' m'') \right] \times F_i(\nu l m; \alpha, \boldsymbol{r}, t) = 0, \quad (36)$$

where $\langle \nu l m || \boldsymbol{c} \cdot \nabla + \boldsymbol{a} \cdot \partial / \partial \boldsymbol{c} || \nu' l' m' \rangle$ is a matrix element containing field and spatial derivative terms, $(l' m' l'' m'' | l m)$ is a Clebsch–Gordan coefficient and $(J_i)_{\nu\nu'}^{l}$ and $(J_{i,i'})_{\nu\nu'\nu''}^{l l' l''}$ are matrix elements of the respective collision operators in (1). All matrix elements are either given explicitly in [15–17], or can be readily calculated using the techniques developed therein. This system of equations is valid in the non-hydrodynamic regime. The quantities of physical interest are given in terms of the solutions $F_i(\nu l m; \alpha, \boldsymbol{r}, t)$ of (36), e.g. the number density $n_i(\boldsymbol{r}, t) = F_i(000)$.

The determination of the matrix elements of the collision operator is central to the calculation, but can be very time consuming and their computation requires attention to accuracy. We refer the reader to [15, 17, 68, 69] for details. It will suffice here to state that we make a general mass ratio m/m_0 (where m_0 is the mass of the neutral gas constituent) expansion of the collision operator:

$$J_{\nu\nu'}^{l} = \sum_{p=0}^{\infty} \left(\frac{m}{m + m_0} \right)^p J_{\nu\nu'}^{l}(p) \quad (37)$$

and truncate the p-summation at a level which satisfies a predefined accuracy criterion. This method for the calculation of the collision matrix elements is valid for arbitrary mass ratios leading to a unified theory for electrons and ion swarms. There is no benefit to assuming *a priori* the small mass ratio forms of the collision operators (e.g. Davydov and Frost–Phelps collision operators traditionally used).

2.3.3. Hydrodynamic regime—density gradient expansion. As detailed above, in the (time-dependent) hydrodynamic regime, the following projection of the implicit space–time dependence onto n and its derivatives is made using a spherical tensor equivalent of (17) for the moments $F(\nu l m; \boldsymbol{r}, t)$

$$F(\nu l m; \boldsymbol{r}, t) = \sum_{s=0}^{\infty} \sum_{\lambda=0}^{\infty} \sum_{\mu=-\lambda}^{\lambda} F(\nu l m | s \lambda \mu; \alpha, t) G_{\mu}^{(s\lambda)} n(\boldsymbol{r}, t), \quad (38)$$

where $G_{\mu}^{(s\lambda)}$ is the irreducible gradient tensor operator [64]. Substitution of (38) into (36), we obtain the following hierarchy of coupled first order differential equations in time for the moments $F(\nu l m | s \lambda \mu; \alpha, t)$ for a field configuration in which $\boldsymbol{E}$ and $\boldsymbol{B}$ are at an angle ψ with respect to each other:

$$\sum_{\nu'=0}^{\infty} \sum_{l'=0}^{\infty} \sum_{m'=-l'}^{l'} \left[\left(\{ n_0 \partial_t - R_a \} \delta_{\nu\nu'} + n_0 J_{\nu\nu'}^{l}(\alpha) \right) \delta_{l'l} \delta_{m'm} + \mathrm{i} \frac{qE}{m} \alpha (l' m 10 | l m) < \nu l || K^{[1]}(\alpha) || \nu' l' > \delta_{m'm} + \frac{qB}{m} \left\{ \sqrt{(l - m)(l + m + 1)} \frac{\sin\psi}{2} \delta_{m' m+1} - \sqrt{(l + m)(l - m + 1)} \frac{\sin\psi}{2} \delta_{m' m-1} - \mathrm{i} m \cos\psi \delta_{m'm} \right\} \times \delta_{\nu\nu'} \delta_{l'l} - (1 - \delta_{s0} \delta_{\lambda 0} \delta_{\mu 0}) n_o J_{0\nu'}^{0}(\alpha) F(\nu l m | 000) \right] \times F(\nu' l' m' | s \lambda \mu) = X(\nu l m | s \lambda \mu), \quad (39)$$

where the explicit expressions for the rhs are given in [33] and R_a is the net particle loss rate

$$R_a = -\sum_{\nu=0}^{\infty} n_0 J_{0\nu}^{0} F(\nu 00 | 000). \quad (40)$$

Symmetry properties for the moments are used to minimize the computational requirements [33]. Solution of (39) for the moments $F(\nu lm|s\lambda\mu)$ allows calculation of all quantities of interest including the velocity distribution function, e.g.

- *Bulk* drift velocity vector components:

$$W_x = \frac{1}{\alpha}\sqrt{2}\,\mathrm{Im}\{F(011|000)\} - \sum_{\nu=0}^{\infty} n_0 J_{0\nu}^0 \sqrt{2}\,\mathrm{Im}\{F(\nu 00|111)\}, \tag{41}$$

$$W_y = \frac{1}{\alpha}\sqrt{2}\mathrm{Re}\{F(011|000)\} + \sum_{\nu=0}^{\infty} n_0 J_{0\nu}^0 \sqrt{2}\,\mathrm{Im}\{F(\nu 00|111)\}, \tag{42}$$

$$W_z = -\frac{1}{\alpha}\,\mathrm{Im}\{F(010|000)\} + \sum_{\nu=0}^{\infty} n_0 J_{0\nu}^0 \sqrt{2}\,\mathrm{Im}\{F(\nu 00|110)\}. \tag{43}$$

- *Bulk* diffusion tensor diagonal elements:

$$D_{xx} = -\frac{1}{\alpha}\Big[\mathrm{Re}\{F(011|111)\} - \mathrm{Re}\{F(01-1|111)\}\Big] - \sum_{\nu=0}^{\infty} n_0 J_{0\nu}^0 \Big[\sqrt{\frac{1}{3}}F(\nu 00|200) + \sqrt{\frac{1}{6}}F(\nu 00|220) - \mathrm{Re}\{F(\nu 00|222)\}\Big], \tag{44}$$

$$D_{yy} = -\frac{1}{\alpha}\Big[\mathrm{Re}\{F(011|111)\} + \mathrm{Re}\{F(01-1|111)\}\Big] - \sum_{\nu=0}^{\infty} n_0 J_{0\nu}^0 \Big[\sqrt{\frac{1}{3}}F(\nu 00|200) + \sqrt{\frac{1}{6}}F(\nu 00|220) + \mathrm{Re}\{F(\nu 00|222)\}\Big], \tag{45}$$

$$D_{zz} = -\frac{1}{\alpha}F(010|110) - \sum_{\nu=0}^{\infty} n_0 J_{0\nu}^0 \Big[\sqrt{\frac{1}{3}}F(\nu 00|200) + \sqrt{\frac{2}{3}}F(\nu 00|220)\Big]. \tag{46}$$

The terms involving the summations in the drift velocity and diffusion tensor elements represent the explicit effects of non-conservative collisions on the bulk transport coefficients discussed previously. Those parts of expressions (41)–(46) not involving the summations are the respective flux transport properties. Note, Re{} and Im{}, respectively, represent the real and imaginary parts of the moments. Expressions for ε, γ, $\boldsymbol{T}$ and off-diagonal elements are available in [24]. The spatially-averaged velocity distribution function is given by:

$$f^{(0)}(\boldsymbol{c}) = \sum_{l=0}^{\infty}\sum_{m=-l}^{l} f(lm|000)Y_m^{[l]}(\hat{\boldsymbol{c}}) = \sum_{l=0}^{\infty}\sum_{m=0}^{l}(2-\delta_{m0})\Big[\mathrm{Re}\{\tilde{F}_{lm}\}\cos(m\phi) - \mathrm{Im}\{\tilde{F}_{lm}\}\sin(m\phi)\Big] \times P_l^{|m|}(\cos\theta), \tag{47}$$

where

$$\tilde{F}_{lm} = i^l(-1)^m\sqrt{\frac{(2l+1)(l-m)!}{4\pi(l+m)!}}f(lm|000). \tag{48}$$

The polar and azimuthal angles of the velocity vector are defined by θ and ϕ respectively while $P_l^{|m|}$ is an associated Legendre polynomial.

2.3.4. Numerical solution of the matrix equations. The solution of (36) in the non-hydrodynamic regime and (39) in the hydrodynamic regime proceeds after truncation to finite size by imposing upper limits on the respective indices, with the 'two-term' approximation corresponding to $l_{\max} = 1$. Indications are that the m-index may be truncated independently [32, 33]. All these indices are then successively incremented until some prescribed accuracy criterion is met [33]. The values of $\nu_{\max}$ vary depending on the basis temperature T_b and schemes are available for the choice of this parameter under time-dependent circumstances [34]. For space and time derivatives various schemes are available. Implicit finite differencing is favoured in time, while various finite differencing schemes have been implemented in space [36, 51]. Sparseness and block structure are exploited whereever possible.

2.3.5. Comparison with other methods. For light particles such as electrons, the non-reactive collision operator (9) is expressible to first order in m/m_0 ($p = 1$ in equation (37)) in differential-finite difference form [70], thus enabling standard solution techniques for differential equation to be employed if desired. In this case it is often seen as preferable to discretize on a mesh of N points in speed space (see, e.g. [37]), rather than proceed via a polynomial expansion. Nevertheless, one still arrives at an equivalent set of matrix equations for which truncation in three indices (N,l,m) is required. Our view is, however, that since one still has to solve the *ion* kinetic equation, where discretization in speed or energy space does not seem viable, it seems preferable to use the polynomial expansion method for *both* the ion and electron components from the outset.

In summary, since the aim is to develop a general method capable of dealing with *all* types of particles in a low-temperature plasma, it seems to us that it is advantageous to use a polynomial expansion for all species, right from the outset. We do not wish to be prescriptive in this regard, but nevertheless stress the need to consider the kinetic theory of *all* components of the plasma together, for that is the actual problem to be faced. To consider only electron kinetic theory in isolation, and to neglect the corresponding problem for ions, is to avoid the true problem of plasma kinetic theory. There exists a wealth of prior literature on swarms (electrons or ions) that will facilitate pursuit of this goal. Finally, we reiterate: whatever solution technique is chosen, one should always be careful to distinguish the range of validity of the equation being solved from the limitations of the numerical routine used to solve it.

3. Fluid modelling

The solution of (1), or equivalently (36) in matrix form, for the full non-hydrodynamic plasma is formidable and a fluid equation treatment is often more tractable. Here the problem of solving the Boltzmann equation for f in phase space is replaced by a low order set of approximate equations for the moments of f. The recent paper [25] is directly aimed at reconciling the swarm and plasma literature with a particular focus on fluids models, their origin and validity.

3.1. General moment equations

The set of moment/balance equations can be found by multiplying (1) by $\phi(\boldsymbol{c})$ and integrating over all velocities

$$\frac{\partial[n\langle\phi(\boldsymbol{c})\rangle]}{\partial t} + \nabla\cdot[n\langle\boldsymbol{c}\phi(\boldsymbol{c})\rangle] - n\frac{q}{m}\left[\left\langle(\boldsymbol{E}+\boldsymbol{c}\times\boldsymbol{B})\cdot\frac{\partial\phi(\boldsymbol{c})}{\partial\boldsymbol{c}}\right\rangle\right] = C_\phi, \tag{49}$$

where C is the collision term in the balance equation and is given generally by:

$$C_\phi = -\int \phi(\boldsymbol{c})J(f)\,\mathrm{d}\boldsymbol{c}. \tag{50}$$

At this stage, the set of equations (49) is exact. A favoured method of modelling plasmas is to use continuity, momentum and energy balance equations i.e. $\phi(\boldsymbol{c}) = 1, m\boldsymbol{c}$ and $1/2mc^2$, respectively:

$$\frac{\partial n}{\partial t} + \nabla\cdot n\boldsymbol{v} = C_1, \tag{51}$$

$$nm\frac{\partial\boldsymbol{v}}{\partial t} + nm\boldsymbol{v}\cdot\nabla\boldsymbol{v} + \nabla\cdot\boldsymbol{P} - nq(\boldsymbol{E}+\boldsymbol{v}\times\boldsymbol{B}) = C_{mc}, \tag{52}$$

$$n\frac{\partial\left(\epsilon - \frac{1}{2}mv^2\right)}{\partial t} + n\boldsymbol{v}\cdot\nabla\left(\epsilon - \frac{1}{2}mv^2\right) + \nabla\cdot\boldsymbol{J}_q + \boldsymbol{P}:\nabla\boldsymbol{v} = C_{\frac{1}{2}mc^2}, \tag{53}$$

where $\boldsymbol{v} = \langle\boldsymbol{c}\rangle$ and $\epsilon = \langle\frac{1}{2}mc^2\rangle$ is the average energy. The heat flux vector and the pressure tensor are defined by $\boldsymbol{J}_q = \frac{1}{2}nm\langle(\boldsymbol{c}-\boldsymbol{v})^2(\boldsymbol{c}-\boldsymbol{v})\rangle$ and $\boldsymbol{P} = nm\langle(\boldsymbol{c}-\boldsymbol{v})(\boldsymbol{c}-\boldsymbol{v})\rangle$ respectively. To solve this system of equations approximations must be made to: (i) close the set of equations (since $\boldsymbol{P}$ and $\boldsymbol{J}_q$ must be obtained from higher order equations) and (ii) evaluate the respective collision terms. It is important that these be done consistently for all species and that some estimate of accuracy can be made.

3.2. Evaluating collision terms—momentum transfer theory

There should be no arbitrariness in the form of the collision terms and further it should be clear how to modify the theory to attain higher accuracy. References [25, 26] have discussed this topic in detail and the various schemes involved and we refer the reader to these references for a comprehensive discussion. We propose here, and elsewhere, the use of momentum transfer theory [12, 22, 71, 72] as a means of evaluating the collision terms and satisfying the above requirements. This method has been used extensively in swarms and we believe its utility and accuracy can carry over to plasmas since the approximations occur only in the collision terms and do not affect the field terms. At its lowest level of approximation (for particle conserving processes) the balance equations are of the same mathematical form as for the constant collision frequency model (point charge induced dipole interactions), but with an energy-dependent collision frequency. For non-conservative processes such as ionization, attachment, ion–molecule reactions, etc. however, the next level of approximation is required involving energy derivatives of the collision frequency [71]. Note that Viehland and co-workers [73–75] employ a type of momentum transfer theory with an explicit form of f assumed, effectively (32) to low order. However, it is neither necessary nor desirable in our opinion to make such an assumption.

Using the momentum transfer approximation, the balance equations (51)–(53) have the form

$$\frac{\partial n}{\partial t} + \nabla\cdot n\boldsymbol{v} = n\,(\nu_\mathrm{I}(\bar\epsilon) - \nu_a(\bar\epsilon)), \tag{54}$$

$$nm\frac{\mathrm{d}\boldsymbol{v}}{\mathrm{d}t} + \nabla\cdot\boldsymbol{P} - nq\,(\boldsymbol{E}+\boldsymbol{v}\times\boldsymbol{B}) = -n\mu\nu_m(\bar\epsilon)\boldsymbol{v} - nm\boldsymbol{v}\left(\nu_\mathrm{I}(\bar\epsilon) + \xi\nu_a'(\bar\epsilon)\right), \tag{55}$$

$$n\frac{\mathrm{d}}{\mathrm{d}t}\left(\epsilon - \tfrac{1}{2}mv^2\right) + \nabla\cdot\boldsymbol{J}_q + \boldsymbol{P}:\nabla\boldsymbol{v} = -n\,\nu_\mathrm{e}(\bar\epsilon)\left[\epsilon - \tfrac{3}{2}kT_0 - \tfrac{1}{2}(m+m_0)v^2 + \Omega(\bar\epsilon)\right] - n\epsilon(\nu_\mathrm{I}(\bar\epsilon) + \xi\nu_a'(\bar\epsilon)) - n\tfrac{1}{2}mv^2(\nu_\mathrm{I}(\bar\epsilon) + \xi\nu_a'(\bar\epsilon)). \tag{56}$$

Here

$$\frac{\mathrm{d}}{\mathrm{d}t} = \frac{\partial}{\partial t} + \boldsymbol{v}\cdot\nabla \tag{57}$$

denotes the convective time derivative and μ is the reduced mass. The average collision frequencies for momentum and energy transfer,

$$\nu_m(\bar\epsilon) = n_0\sqrt{\frac{2\epsilon}{\mu}}\sigma_\mathrm{m}\,(\bar\epsilon) \tag{58}$$

$$\nu_\mathrm{e}(\bar\epsilon) = \frac{2\mu}{(m+m_0)}\,\nu_m(\bar\epsilon), \tag{59}$$

are prescribed functions of the mean energy in the centre-of-mass frame

$$\bar\epsilon = \frac{m_0\epsilon + m\,\frac{3}{2}kT_0}{m+m_0}, \tag{60}$$

where k is Boltzmann's constant, T_0 is the neutral gas temperature and dashed quantities represent energy derivatives. The attachment and total ionization collision frequencies are given by $\nu_a(\bar\epsilon)$ and

$$\nu_\mathrm{I} = \sum_i \nu_\mathrm{I}^{(i)}, \tag{61}$$

respectively, where we have summed over all possible channels i, in which ions are produced in excited states characterized by energies $\epsilon_I^{(i)}$. The term Ω represents the average energy lost in

one collisional energy relaxation time ν_e^{-1}, through non-elastic processes and is given by

$$\Omega = \frac{m_0}{m+m_0}\sum_\alpha \epsilon_\alpha \frac{\overrightarrow{\nu_\alpha} - \overleftarrow{\nu_\alpha}}{\nu_e(\bar{\epsilon})} - \sum_i \Delta\epsilon_I^{(i)} \frac{\nu_I^{(i)}}{\nu_e(\bar{\epsilon})}. \quad (62)$$

The inelastic channels α are governed by threshold energies ϵ_α and collision frequencies for inelastic and superelastic processes $\overrightarrow{\nu_\alpha}$ and $\overleftarrow{\nu_\alpha}$ respectively. The latter are also prescribed functions of $\bar{\epsilon}$ but need to be specified more carefully in terms of the corresponding cross sections, $\sigma_I(\bar{\epsilon})$.

3.3. Solutions regimes and closure assumptions

The closure of the system of equations (54)–(56) requires approximations or assumptions on the form and/or magnitude of both $\boldsymbol{J}_q$ and $\boldsymbol{P}$ since both must otherwise be obtained from higher order moment equations (which in turn involves higher order unknown moments). The level of approximation is dependent on the solution regime that we are studying. Although our theory is valid for all mass ratios and all collisional processes, for simplicity, in what follows we will consider light particles ($m/m_0 \ll 1$) undergoing only particle conserving collisions only. The reader is referred to [71] for the more general cases. For light particles, $\bar{\epsilon} \approx \epsilon \gg \frac{1}{2}mv^2$, and the pressure temperature simplifies to

$$\boldsymbol{P} = nk\boldsymbol{T} \approx \tfrac{2}{3}n\epsilon\boldsymbol{I}. \quad (63)$$

Treatment of the heat flux vector however remains a little more pivotal and dependent on the regime under investigation.

3.3.1. Time-dependent hydrodynamic regime. As detailed in section 2.2, in the weak-gradient hydrodynamic regime a sufficient representation of the space-(implicit) time dependence of the phase space distribution and all velocity moments is the density gradient expansion (17). The following system of equations for the hydrodynamic transport properties then follow:

- Spatially homogeneous equations:

$$\frac{\mathrm{d}\boldsymbol{W}_\mathrm{F}}{\mathrm{d}t} + \nu_m(\varepsilon)\boldsymbol{W}_\mathrm{F} = \frac{q}{\mu}\left[\boldsymbol{E}(t) + \boldsymbol{W}_\mathrm{F}\times\boldsymbol{B}(t)\right], \quad (64)$$

$$\frac{\mathrm{d}\varepsilon}{\mathrm{d}t} + \nu_e(\varepsilon)\left[\varepsilon - \tfrac{3}{2}kT_0 - \tfrac{1}{2}m_0(W_\mathrm{F})^2 + \Omega(\varepsilon)\right] = 0. \quad (65)$$

- First order inhomogeneous equations:

$$\frac{\mathrm{d}\boldsymbol{D}_\mathrm{F}}{\mathrm{d}t} + \nu_m(\varepsilon)\boldsymbol{D}_\mathrm{F} = \frac{q}{m}[\boldsymbol{D}_\mathrm{F}\times\boldsymbol{B}] + \frac{k\boldsymbol{T}}{m} + \nu_m'(\varepsilon)\boldsymbol{W}_\mathrm{F}\gamma, \quad (66)$$

$$\frac{\mathrm{d}\gamma}{\mathrm{d}t} + \nu_e(\varepsilon)\left[1 + \Omega'(\varepsilon) - \frac{\mathrm{d}\varepsilon}{\mathrm{d}t}\frac{\nu_e'}{\nu_e^2}\right]\gamma = -m_0\boldsymbol{W}_\mathrm{F}\cdot\boldsymbol{D}_\mathrm{F} - \boldsymbol{J}_q \quad (67)$$

.

These equations can be generalized for non-conservative processes [35]. Equations (64) and (65) represent coupled non-linear differential equations for $\boldsymbol{W}_\mathrm{F}$ and ε, which when solved, permit solutions of the linear coupled differential equations for $\boldsymbol{D}_\mathrm{F}$ and γ once a closure assumption is made on the spatially homogeneous component of the heat flux $\boldsymbol{J}_q$. In general, under hydrodynamic conditions this term is safe to neglect although there are exceptions [76].

From this system of equations one can reproduce known relations/results from swarm physics such as Wannier's energy relation, generalized Einstein relations [71, 22], Tonk's theorem [77], equivalent electric field concept (when magnetic fields are considered) [78], Blanc's law (mixtures), effective dc field (when rf electric fields are present) [79] and many others [25, 35, 71, 80].

3.3.2. Non-hydrodynamic regime—light particles. Under non-hydrodynamic conditions, (55)–(56) in the limit of light particles reduce to

$$nm\frac{\mathrm{d}\boldsymbol{v}}{\mathrm{d}t} + \frac{2}{3}\nabla(n\epsilon) - nq(\boldsymbol{E} + \boldsymbol{v}\times\boldsymbol{B}) = -nm\nu_m(\epsilon)\boldsymbol{v} \quad (68)$$

and

$$n\frac{\mathrm{d}\epsilon}{\mathrm{d}t} + \nabla\cdot\boldsymbol{J}_q + \tfrac{2}{3}n\epsilon\nabla\cdot\boldsymbol{v} = -n\nu_e(\epsilon)\left[\epsilon - \tfrac{3}{2}kT_0 - \tfrac{1}{2}m_0v^2 + \Omega(\epsilon)\right]. \quad (69)$$

Some *ansatz* (postulate) is needed to close the set which in this case means somehow specifying the heat flux $\boldsymbol{J}_q$ in terms of lower order moments n, ϵ and $\boldsymbol{v}$. This question is crucial for the success of the fluid model, but is all too often dealt with in a cursory, ad hoc or totally unphysical way in the plasma literature. In [25, 81] a new ansatz is proposed which, as with momentum transfer theory, is chosen to be exact for a particular model and is benchmarked against known results for other models.

4. Results and discussion

With the highly applied nature of the field of plasma processing, modelling of the complex electron and ion kinetics in low-temperature plasma discharges is inevitably driven by computational efficiencies. For fluid and kinetic models of plasmas, fundamental questions of scientific rigour often arise regarding the foundations of the balance equations or the 'Boltzmann equation' employed. In addition, solution of these models often involve assumptions and/or approximations and naturally questions of validity and accuracy arise here as well. For this reason, the swarm limit plays an important role through the provision of benchmarks for low-temperature plasma models in the free diffusion limit. It also facilitates the extraction of underlying fundamental physical transport processes without the added complication of space-charge fields. Further, swarm transport properties are often used as input data for fluid models as a means of evaluating the collision transfer terms in the balance equations. For these reasons, we shall focus on the swarm limit in the rest of this section. The swarm–plasma nexus is further detailed in [25, 26] and in the companion paper of Petrovic *et al* in this issue.

We have developed Boltzmann equation and momentum transfer theory solutions capable of handling (i) all types collisional processes, (ii) arbitrarily oriented electric and

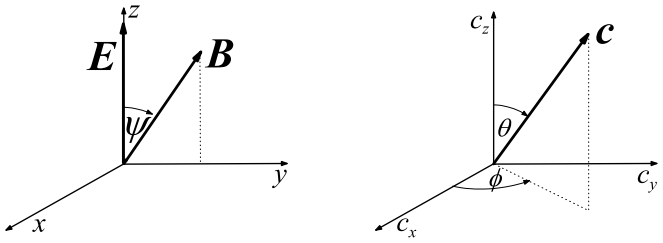

Figure 2. Configuration and velocity space coordinate systems together with field orientations employed in this study.

magnetic fields and (iii) arbitrary time-dependence of the electric and magnetic fields. The theories and associated codes are valid for both electrons and ions. For the Boltzmann equation solutions, no restrictions are imposed on the anisotropy of the velocity distribution function nor on the anisotropy of the cross sections. The codes have been systematically benchmarked against independent Monte Carlo simulations and other techniques where possible under both dc and time-dependent conditions (see, e.g. [24, 30, 32, 82]).

Swarm transport coefficients in dc electric and/or magnetic fields have been reviewed extensively and we refer the reader to [24, 28, 30, 31, 32, 39] for a detailed discussion. In the paper, we will focus attention on two important issues in low-temperature plasma modelling, namely the treatment of temporal and spatial non-locality. In what follows we consider both Boltzmann equation and fluid equation treatments, highlighting significant phenomena, assessing accuracy of approximations and demonstrating the generality of the theories outlined. Further, we assess the accuracy of the momentum transfer theory fluid equation treatment through direct comparison with multi-term Boltzmann equation results where possible.

In this work we employ the velocity and configuration space coordinate systems detailed in figure 2 along with the assigned field conventions. Electric and magnetic field strengths are presented in units of townsends (1 Td = 10^{-21} V m^2) and Huxley (1 Hx = 10^{-27} T m^3) respectively. In the general case where $\boldsymbol{E}$ and $\boldsymbol{B}$ are crossed at an arbitrary angle ψ, vector (e.g. $\boldsymbol{W}, \gamma$) and tensorial (e.g. $\boldsymbol{D}, \boldsymbol{T}$) transport properties are full. For parallel fields, $\psi = 0$, the drift velocity vector and diffusion tensor (and properties of equal rank) have the following form:

$$\boldsymbol{W} = \begin{pmatrix} 0 \\ 0 \\ W_z \end{pmatrix}; \qquad \boldsymbol{D} = \begin{pmatrix} D_{xx} & D_{xy} & 0 \\ -D_{xy} & D_{xx} & 0 \\ 0 & 0 & D_{zz} \end{pmatrix}, \tag{70}$$

while for orthogonal fields, $\psi = \pi/2$, they reduce to the well-known expressions:

$$\boldsymbol{W} = \begin{pmatrix} W_x \\ 0 \\ W_z \end{pmatrix}; \qquad \boldsymbol{D} = \begin{pmatrix} D_{xx} & 0 & D_{xz} \\ 0 & D_{yy} & 0 \\ D_{zx} & 0 & D_{zz} \end{pmatrix}. \tag{71}$$

4.1. Temporal non-locality

In this section we consider the time-resolved hydrodynamic transport properties under the action of time-varying electric and/or magnetic fields emphasizing the non-locality in time of the transport properties. We will focus on two particular systems: (i) the temporal response to the application of a magnetic field and (ii) radiofrequency fields.

4.1.1. Transient response of electrons in E and B fields. In this section we examine the explicit impact of magnetic fields on the transient response of transport properties. The arrangement initially considered in [83] and extended in [82] has a steady state swarm under the action of an electric field at time $t = 0$ subject to a magnetic field (electric field remaining unaltered). The relaxation of the swarm properties is monitored as a function of time (normalized time is $n_0 t$). The results are displayed in figure 3 for electrons in CO_2 over a range of B/n_0 for the orthogonal field configuration.

In the relaxation profiles we observe the existence of three distinct timescales: (i) the gyro-period of the electrons τ, (ii) the momentum relaxation time τ_m and (iii) the energy relaxation time τ_e. The latter two timescales are functions of energy. We observe that for scalar transport properties, or those components of properties parallel to the magnetic field (e.g. ε and $n_0 D_{yy}$), relaxation is in general monotonic and occurs on a timescale governed by τ_e . In contrast, those quantities with components perpendicular to the magnetic field (e.g. drift and diffusion in the $\boldsymbol{E}\,(z)$ and $\boldsymbol{E} \times \boldsymbol{B}\,(x)$ directions) exhibit a transition from monotonic decay to damped periodic decay as the magnetic field strength is increased to values where $\tau \leqslant \tau_m$. For the damped periodic profiles, the period of oscillations is governed by the gyro-period τ and the envelope decays on a timescale of τ_m together with a further relaxation on the timescale of τ_e. The existence of the additional oscillatory behaviour in the relaxation profiles is a reflection of the collective gyrations of the electrons damped by collisions that exchange momentum and energy. Perhaps the most striking phenomenon is the existence of transiently negative deviations of the diffusion tensor elements in both the $\boldsymbol{E}$ and $\boldsymbol{E} \times \boldsymbol{B}$ directions. Such behaviour was initially observed by the Belgrade group [29] for $n_0 D_{xx}$ when considering radiofrequency electric and magnetic fields. This was independently verified by the JCU group [24] and shown to exist in $n_0 D_{zz}$ as well. The results in figure 3 indicate that transiently negative diffusion in both the E and $E \times B$ directions can be achieved through the abrupt application of a dc magnetic field of sufficient strength.

We now consider the more general case where the magnetic field is crossed at an arbitrary angle ψ to the electric field. In figure 4, transport properties are presented as a function of ψ for a fixed value of B/n_0. The temporal profiles are highly sensitive to the angle between the fields. Although scalar properties still relax monotonically, $n_0 D_{yy}$ now has an oscillatory nature for $\psi \neq 0, \pi/2$. This oscillatory nature is reduced as ψ increases contrasting that for $n_0 D_{zz}$ and reflecting oscillations in the plane orthogonal to $\boldsymbol{B}$ associated with the Lorentz force. Importantly we see from figure 4 that the application of a non-orthogonal magnetic field generates off-diagonal elements of the diffusion tensor which are of the same order of magnitude as the diagonal components. One observes that in contrast to the diagonal elements of the diffusion tensor,

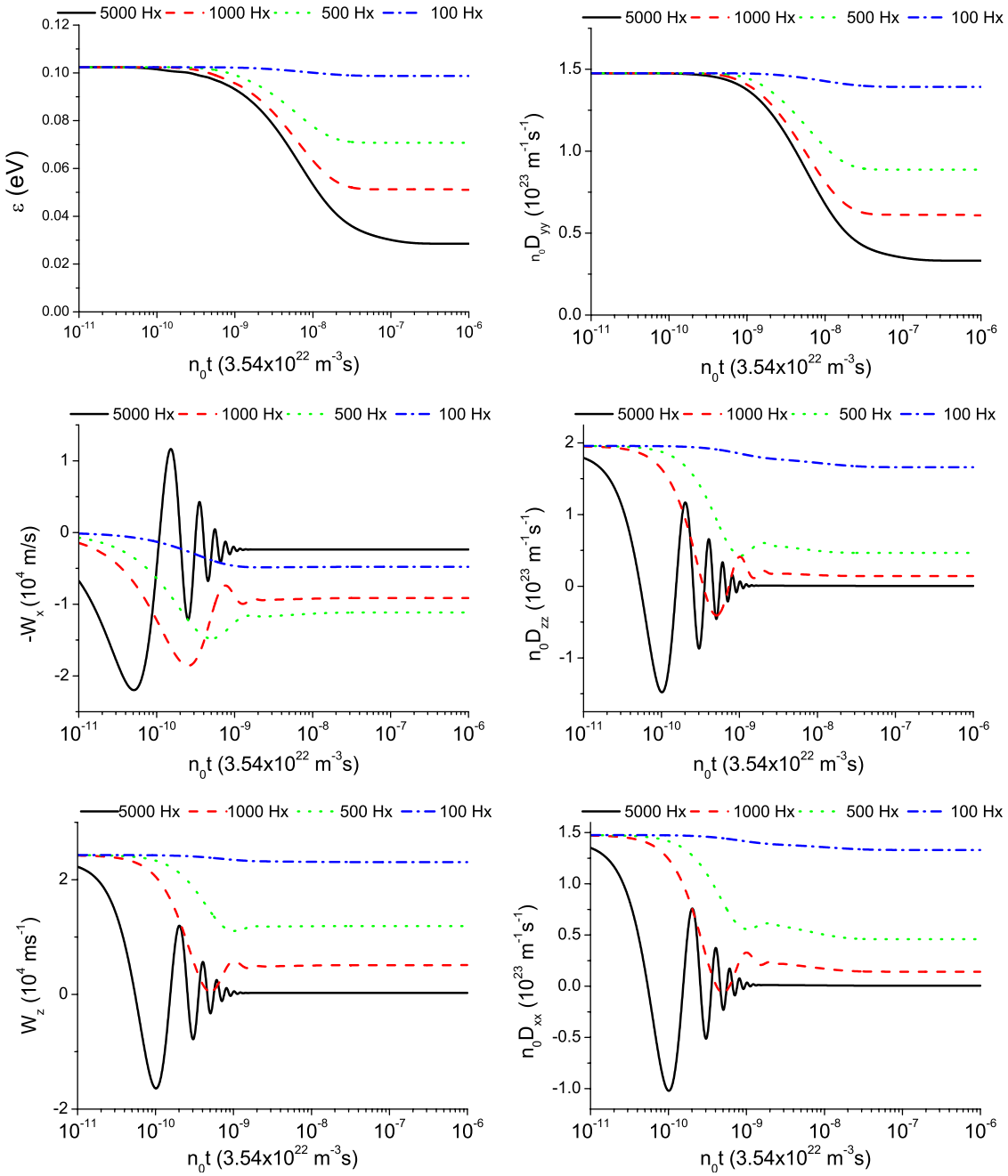

Figure 3. Temporal relaxation of the mean energy, drift velocity and diagonal elements of the diffusion tensor for various crossed magnetic fields for electrons in CO_2 using the set of cross sections developed in [93] ($E/n_0 = 5$ Td, $T_0 = 293$ K).

for the fields considered, the off-diagonal elements do not exhibit the signature oscillations on the timescale of the gyro-orbit, although as B/n_0 increases the damped oscillatory type relaxation does indeed develop (not shown here). The drift velocity vector and diffusion tensor are clearly anisotropic and full and have different transient responses to the application of a magnetic field. Such behaviour should be accounted for when implementing such data in plasma fluid models, and can also have important manifestations when considering time-varying fields [85].

In figure 4 we also compare the results obtained from a multi-term solution of the Boltzmann equation with those using the two-term approximation. We find $l_{\max} = 4$ is required in order to achieve convergence of the transport properties over the transient profiles to within the specified accuracy of 0.5% . The large cross sections for vibrational excitations in CO_2 are known to produce asymmetry of f in velocity space. Consequently, for dc electric fields (i.e. the initial condition), the two term approximation can be in error by as much as 20%. The application of an orthogonal component of the magnetic field impacts upon the accuracy of two-term approximation in various ways for the various coefficients. For certain coefficients, the accuracy of the two-term approximation is enhanced while for others it is reduced (see, e.g. errors of 50% are observed for $n_0 D_{yz}$), indicating that it can enhance or inhibit isotropy in velocity space in various directions. This

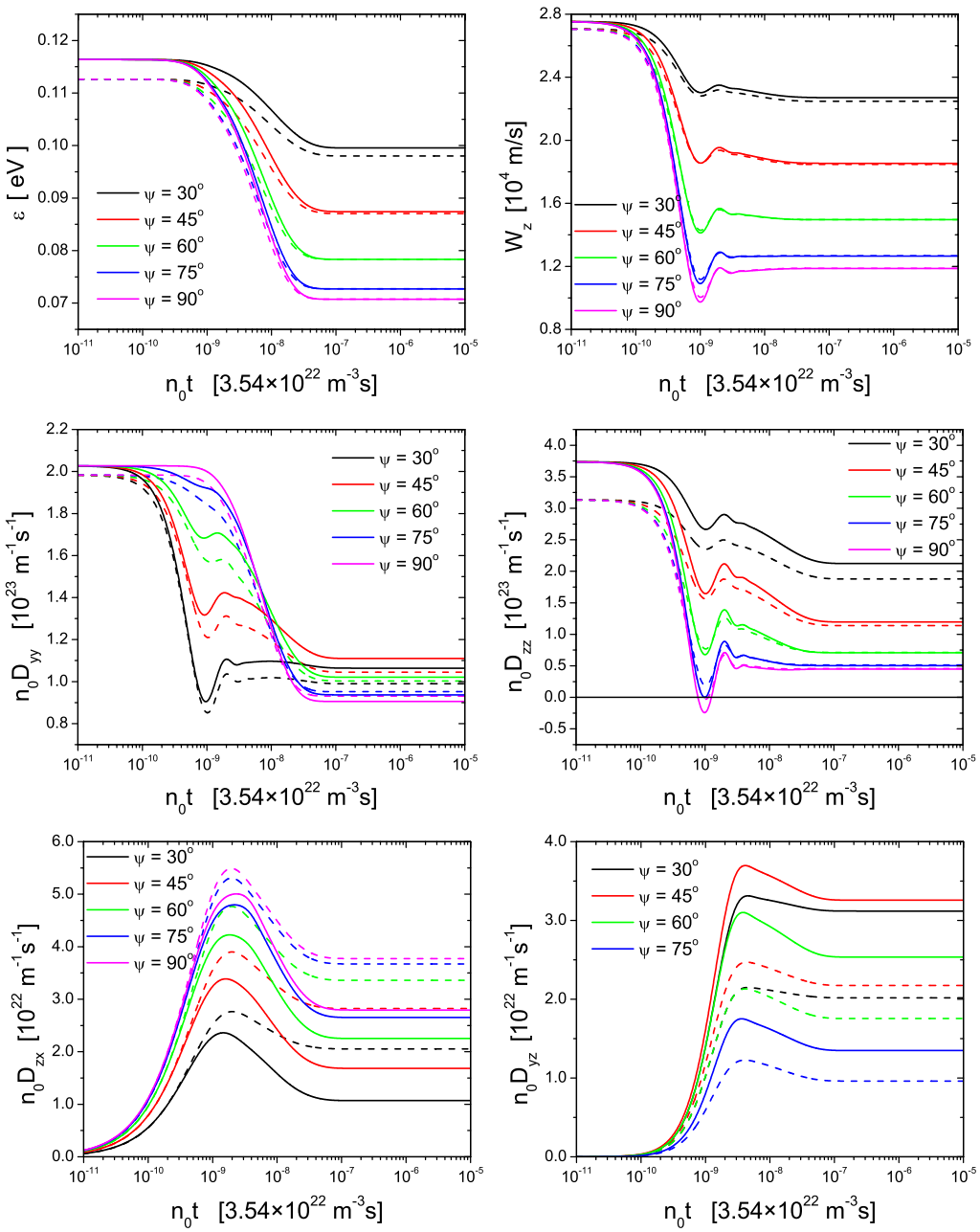

Figure 4. Impact of the magnetic field angle ψ on the temporal relaxation of the transport properties of electrons in CO_2 (E/n_0: 12 Td, $T_0 = 293$ K, B/n_0: 500 Hx (rows 1,2), 100 Hx (row 3)). (dashed lines: two term approximation; full lines: multi-term theory)

is demonstrated in figure 5 where we demonstrate the impact of an orthogonal magnetic field on the velocity distribution function by slicing it in various planes. At $t = 0$ we can clearly see (i) anisotropy of the velocity distribution in the direction of electric field force and (ii) rotational symmetry in velocity space about the electric field direction. In the long-time limit, we observe that the application of an orthogonal magnetic field destroys the symmetry—in fact there is no axis of symmetry in the velocity distribution, emphasizing the futility of a Legendre polynomial expansion in velocity space: a full spherical harmonic expansion of the velocity distribution is generally required. For further details on the impact of magnetic fields on the velocity distribution the reader is referred to [84, 85].

To conclude this section, we consider the fluid equation treatment of the same problem. A numerical solution of the balance equations (64)–(67) using a Newton–Raphson technique has been implemented for electrons in a gas of cold hard spheres for simplicity. The results are presented in figure 6. We note that standard momentum transfer theory is capable of reproducing all qualitative features in the profiles including transiently negative diagonal diffusion coefficients observed for the Boltzmann equation solutions.

In summary, the transient response of drift and diffusion in the $\boldsymbol{E}$, $\boldsymbol{E}\times\boldsymbol{B}$ and $\boldsymbol{E}\times(\boldsymbol{E}\times\boldsymbol{B})$ (y) directions to a magnetic field is in general not predictable from steady state dc results. The manifestation of these complex relaxation profiles when considering time-dependent fields (e.g. rf and/or pulsed rf) is

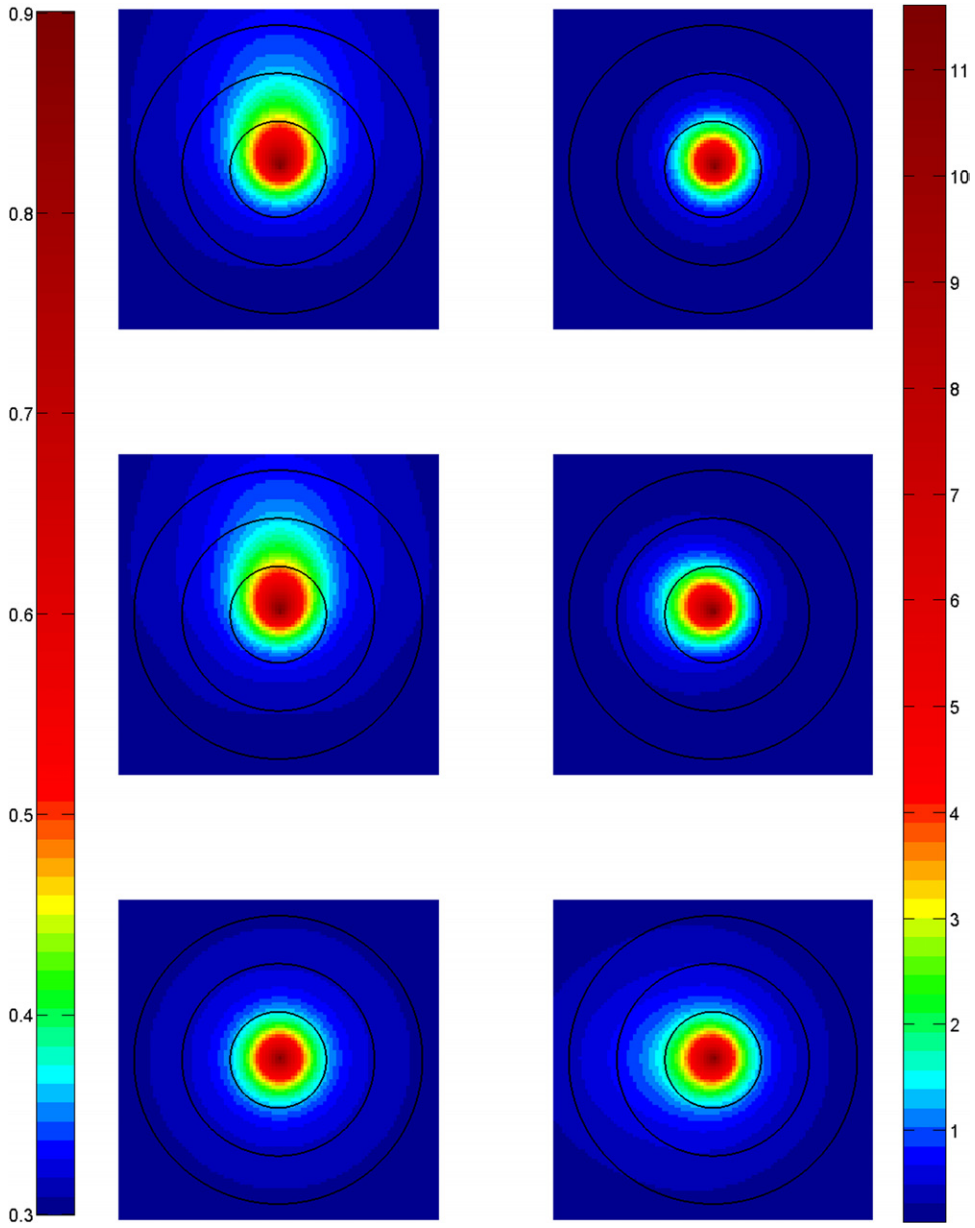

Figure 5. Contour plots of the initial and final velocity distribution functions for electrons in CO_2 in various planes. Row 1: $\phi = 0, \pi$; row 2: $\phi = \pi/2, 3\pi/2$; row 3: $\theta = \pi/2$. Left column and colourbar: initial distribution $B/n_0 = 0$ Hx, Right Column and colourbar: final distribution $B/n_0 = 200$ Hx. The energy scale is indicated by the dashed concentric circular plots of increasing radii referring to 0.3, 0.6 and 0.9 eV, respectively. ($E/n_0 = 5$ Td, $T_0 = 293$ K).

behaviour which is distinctly non-local in time. Contemporary understanding of field frequency effects (namely, reduction in amplitude and increase in phase-lag with respect to the field) fail or have a limited range of validity when the relaxation is not monotonic. Understanding such effects requires recourse to a systematic investigation of relaxation profiles such as those presented here [85].

4.1.2. RF electric and magnetic fields. Recent developments in plasma processing using magnetically controlled rf discharges has led to a renewed interest in the understanding of electron kinetics in radiofrequency electric and magnetic fields. The groups at Belgrade, Greifswald, JCU and others have addressed this problem in considerable detail (see, e.g. [24, 29, 30, 38, 39, 40, 86] These studies have unearthed a variety of new and unexpected phenomena and in what follows we highlight but a few of them.

One of the more interesting phenomena to come out of these studies has been that of anomalous anisotropic diffusion [30, 40, 86]. For dc electric fields only, one may solve the coupled equations (66) and (67) to yield the following form of the generalized Einstein relations [22]:

$$\frac{D_{\mathrm{L}}}{D_{\mathrm{T}}} = \frac{T_{\mathrm{L}}}{T_{\mathrm{T}}} \frac{\partial \ln W}{\partial \ln E} \tag{72}$$

$$= \frac{T_{\mathrm{L}}}{T_{\mathrm{T}}} + \frac{\mu \nu_m' \gamma W}{k T_{\mathrm{T}}}, \tag{73}$$

where $D_{\mathrm{L}} = D_{zz}$ and $D_{\mathrm{T}} = D_{xx} = D_{yy}$ are the longitudinal and transverse diffusion coefficients. Thus physically, the

sources of anisotropic diffusion in dc electric fields only are [85]:

(a) Thermal anisotropy ($T_L \neq T_T$): dispersion of charged particles associated with random motions is different in the directions parallel and perpendicular to $\boldsymbol{E}$;
(b) Differential velocity effect: the spatial variation of local average velocities through the swarm combined with an energy dependent collision frequency act to influence the spread of the swarm parallel to field [87, 86].

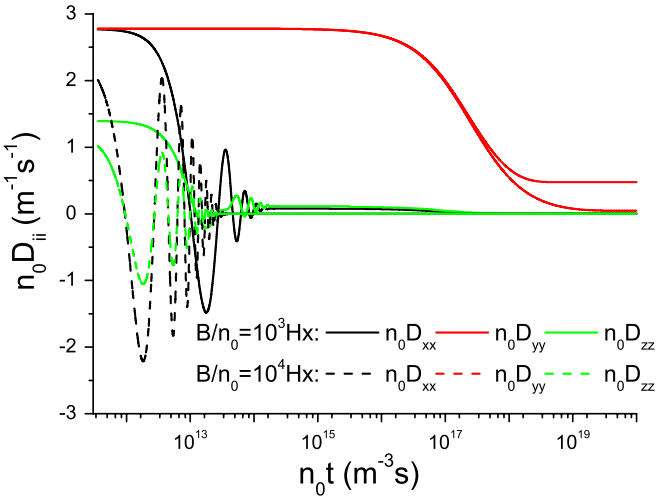

Figure 6. Temporal relaxation of the diagonal elements of the diffusion tensor for various crossed magnetic fields for electrons in a gas of hard spheres using standard momentum transfer theory ($E/n_0 = 1$ Td, $\sigma_m = 6$ Å^2, $T_0 = 0$ K).

For the simple case of electrons in a gas of hard spheres with $T_L \approx T_T$, we can see from (72) that $D_L/D_T \approx 0.5$ (actual value is 0.492).

When one applies a radiofrequency electric field to the system interesting anomalous behaviour in the diffusion coefficients emerges as shown in figure 7. The signature effects for 'anomalous anisotropic diffusion' are [34]:

- At low frequencies we observe the evolution of a spike in the low field phase of the cycle. As the frequency increases the height and temporal extent of the spike are increased until it becomes the dominant feature in the temporal profile of D_L;
- There exist phases in the field where $D_L/D_T \neq 0.5$ and indeed cases where $D_L > D_T$ in contrast to the dc steady state case. The fraction of the field where the latter relation holds increases with increasing frequency until they are anti-phase. Instantaneously for a given frequency diffusion is isotropic four times per cycle;
- In a cycle averaged sense, D_L/D_T increases from 0.5 at low frequencies to 1 at high frequencies.

It is interesting in this case that diffusion is instantaneously isotropic at those phases of the field where drift velocity is zero and the first order spatial variation of the average energy, as characterized by γ, is zero. The phases of the field where $D_L > D_T$ correspond to phases where $\gamma(t)W(t) > 0$. Due to the differences in the timescales for energy and momentum exchange, γ and W do not respond to a change in the field direction on the same timescale [88]. From (73), one can see in these phases that the differential velocity effect now acts to enhance longitudinal diffusion [85, 86] and consequently $D_L > D_T$. To fully understand this phenomenon one needs

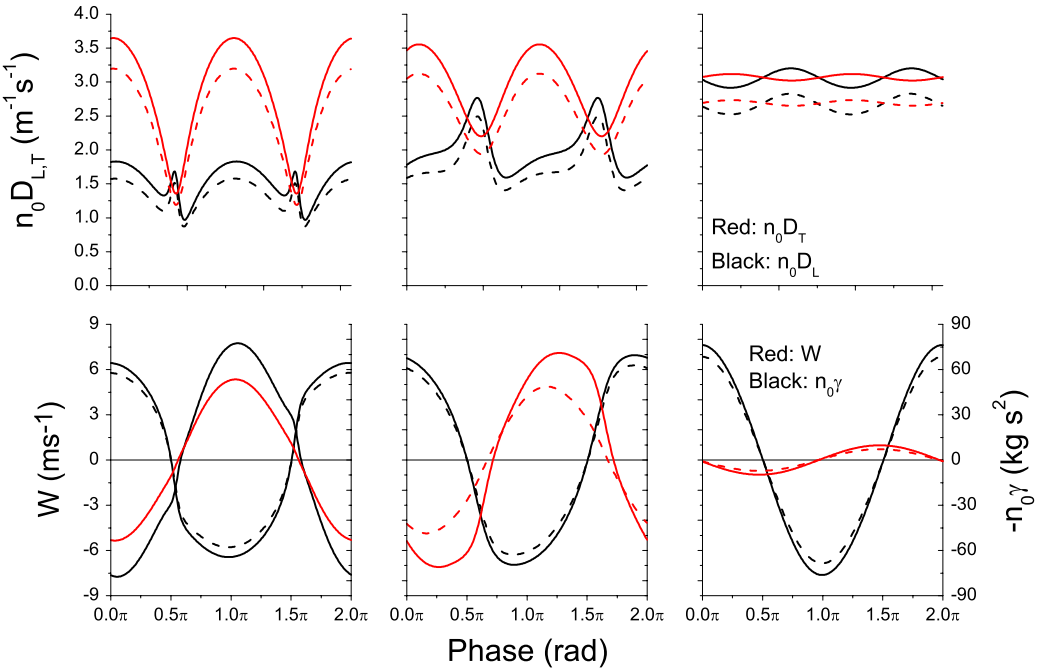

Figure 7. A comparison between standard momentum transfer theory (solid lines) and full time-dependent multi-term solution of Boltzmann equation (dashed lines) for various transport coefficients over a range of reduced angular frequencies ω/n_o for a gas of hard spheres. ($E/n_0 = 1 \cos \omega t$ Td, $\sigma_m = 5$ Å^2, $T_0 = 0$ K, $m_0 = 4$ amu; applied frequencies ω/n_0 (rad m^3 s^{-1}): Col1—1×10^{-18}, Col2—5×10^{-18}, Col3—1×10^{-16}).

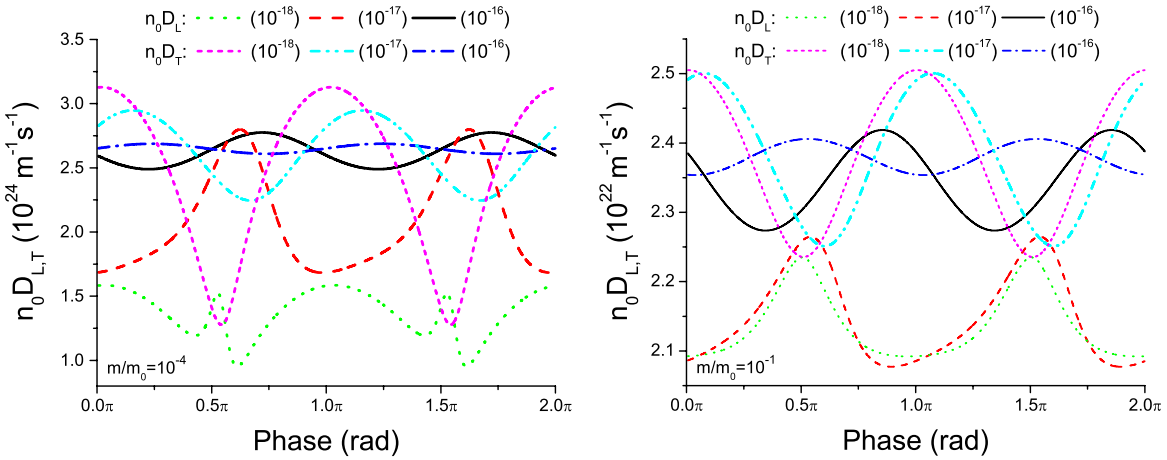

Figure 8. Time-dependent multi-term solution of Boltzmann's equation for the periodic steady state profiles of $n_0 D_L$ and $n_0 D_T$ for various reduced angular frequencies ω/n_0 (in brackets—units $m^3\,s^{-1}$) for two different mass ratios $m/m_0 = 10^{-4}, 10^{-1}$. ($E/n_0 = 1\cos\omega t$ Td, $\sigma_m = 6\,Å^2$, $T_0 = 0\,K$).

to understand and implement the temporal relaxation profiles (for electric fields) such as those considered above [85].

To highlight the effects for ion transport in radiofrequency electric fields, we present and compare in figure 8 the results for two different mass ratio m/m_0 of 10^{-4} and 10^{-1}. For $m/m_0 = 0.1$, we increment the upper bound in the mass ratio expansion of the collision matrix elements (37) until convergence is achieved. For this larger mass ratio of 10^{-1}, although there is different (quasi-) dc behaviour, we note that there is no longer the signature anomalous spike in the D_L profile. The timescales for energy and momentum exchange are no longer distinctly separated for this mass ratio and consequently there is no longer the separation in response times of γ and W required for anomalous diffusion. In addition, thermal anisotropy exists with $T_L > T_T$ and there are now two separate contributing effects to anisotropic diffusion.

To conclude this section on transport in radiofrequency electric fields we now consider the accuracy of a fluid model treatment of this problem. We again consider the numerical solution of (64)–(67), and the results are presented in figure 7 for all coefficients over a range of field frequencies. The fluid model using standard momentum transfer theory is able to reproduce all relevant qualitative features of the Boltzmann equation results including the phenomenon of anomalous anisotropic diffusion. Accuracies again appear to be within about 10-20%. One can improve the accuracy of the scheme by implementing the lookup table approach detailed in [25, 88]. In this procedure, we replace approximate collision frequencies by dc swarm transport coefficients (measured or calculated) and thus avoid the approximations associated with conventional momentum transfer theory. The associated improvement in agreement with the full Boltzmann solution is evident in figure 9 and emphasizes the potential of the technique for improved accuracy. Similar schemes have been utilized elsewhere [89] and the RCT (relaxation continuum theory) model is of particular note [90, 91].

Figure 10 illustrates the Tagashira–Sakai–Sakamoto (TSS) effect on the drift velocity of electrons under conditions of strong electron attachment. We employ the simple attachment benchmark model [56] where attachment collision frequency increases with energy. For the low-frequency quasi-dc regime we find that the bulk drift velocity is instantaneously less than the flux drift velocity. The origin of this effect is well understood and is a consequence of the retardation of the centre-of-mass brought about by preferential attachment of the higher energy electrons at the front of the swarm. In the high frequency regime we note that the TSS effect is reduced/non-existent. In this regime, the frequency of the field is such that the first order spatial variation of the average energy γ cannot respond to changes in the field and the swarm essentially has a symmetric energy profile. As a consequence, there is no preferential spatial attachment through the swarm and the two drift velocities coincide. At intermediate frequencies, however, we have a somewhat counter-intuitive effect, namely the phase lead of the bulk drift velocity, where the bulk drift velocity changes sign before the field changes sign. The origin of this behaviour is the same as for anomalous anisotropic diffusion. The difference in timescales for energy and momentum exchange leads to the situation where although the field is reducing in magnitude (and so too the flux drift velocity), the first order spatial variation in the average energy γ (and hence non-symmetric spatial variation in the attachment processes) is still high, and the rate of change of the centre-of-mass of the swarm due to the loss processes is now greater than the velocity of the centre-of-mass brought about by the field. The bulk drift velocity then changes sign before the field (and flux drift velocity) and the phase lead then follows. This behaviour again is not predictable from traditional descriptions of rf behaviour nor from dc swarm data.

In figure 11 we now consider the impact of an orthogonal rf magnetic field applied out of phase by $\pi/2$ with respect to the electric field, focusing on the drift in the electric field direction. Interestingly we note that the application of the orthogonal rf magnetic field acts to induce, and indeed enhance with increasing magnetic field, a resonance type structure in the profiles around the phase where $B(t) = 0$. As detailed above, the TSS effect arises due to the non-symmetric attachment of electrons caused by a first order spatial variation in the average

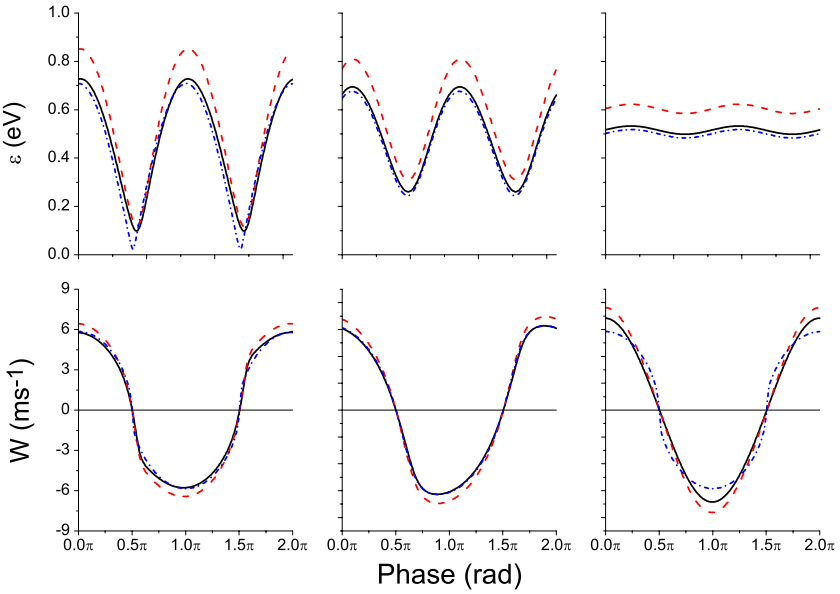

Figure 9. A comparison between the standard momentum transfer theory (dashed), modified momentum transfer theory using look-up dc data (dotted) and a full multi-term solution of the Boltzmann equation (full) for the drift velocity and mean energy for the model in figure 7.

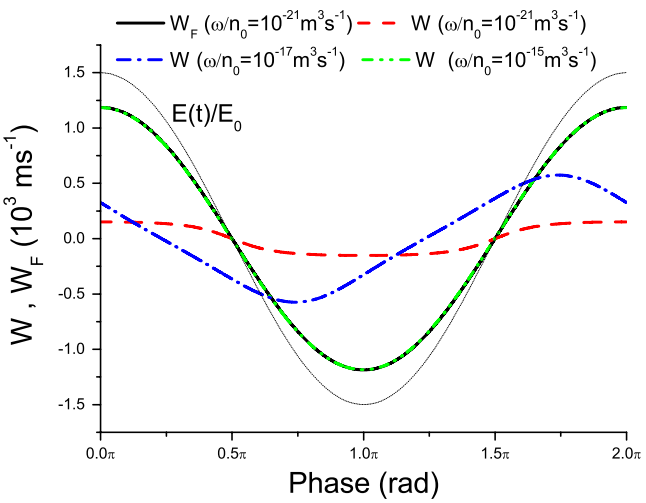

Figure 10. Frequency dependence of the instantaneous TSS effect for the drift velocity in a radiofrequency electric field using the attachment model [56]. Note: the instantaneous flux drift velocity profiles do vary appreciably over this range of frequencies and for clarity only the low-frequency case is presented. ($E/n_0 = 0.4\cos\omega t$ Td, attachment amplitude: 0.1 Å^2 eV$^{-1/2}$, power law: $p = 0.5$).

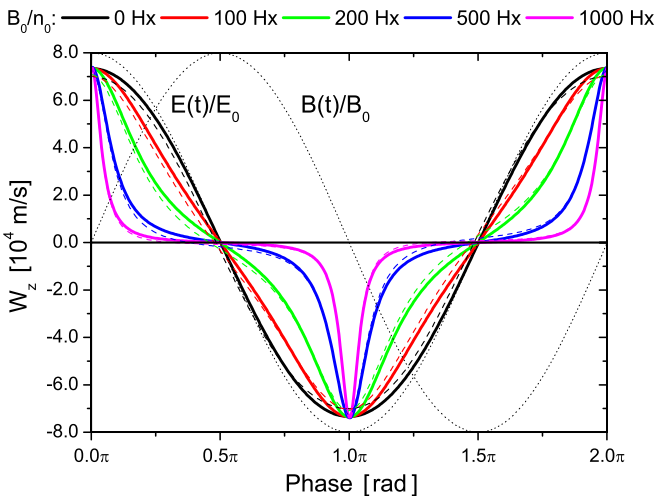

Figure 11. TSS effects for W_z as a function of magnetic field amplitude for orthogonal radiofrequency electric and magnetic fields out of phase by $\pi/2$ using the modified attachment model [30]. The solid and dashed lines represent the flux and bulk temporal profiles respectively. ($E/n_0 = 10\cos\omega t$ Td, $B/n_0 = B_0 \sin\omega t$ Td, ω/n_0: 10^{-16} m^3 s^{-1}, attachment amplitude: 0.5 Å^2 eV$^{-1/2}$, power law: $p = 0.5$).

energy through the swarm. In this case, the rf orthogonal magnetic field reduces γ_z which in turn acts to reduce the explicit TSS effect on the amplitude, although there are again phase-delay effects with respect to the flux drift velocity. Interestingly, in the $\boldsymbol{E} \times \boldsymbol{B}$ direction the spatial variations are essentially symmetric (γ_x is very small) and the TSS effect is minimal in this direction.

4.2. Spatial non-locality—Steady state Townsend and Franck–Hertz experiments

The idealized steady state Townsend (SST) experiment consists of an infinite plane cathode source emitting electrons at a steady rate into a gas in equilibrium. The anode is at a large distance from the source, effectively at infinity, and there is a static, uniform electric field $\boldsymbol{E}$ directed normal to the electrodes, and possibly a magnetostatic field $\boldsymbol{B}$ perpendicular to $\boldsymbol{E}$ (see figure 12). The system eventually reaches a steady state, in which the rate of emission from the source is balanced by the diffusion away from the source. The *essence* of the seminal experiment of Franck and Hertz ([92]) is embodied in the SST experiment (with $B = 0$), for although in the actual experiment there is a grid placed before the anode, this grid is supposed to act in a non-intrusive way, by passing through only electrons above a certain energy without actually perturbing the

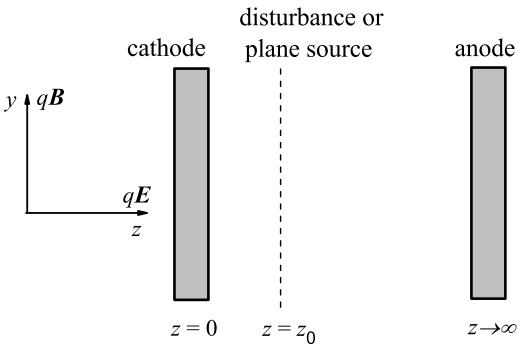

Figure 12. Schematic representation of the idealized state-state Townsend experiment. Charged particles emitted at a constant rate from an infinite plane source at $z = z_0$ interact with the background neutral gas under static external electric and magnetic fields and evolve downstream $z \geqslant z_0$.

distribution function. The current I_a measured at the anode, plotted as a function of the anode voltage V_a is meant to reflect the properties of free electrons in the gas in the Franck–Hertz chamber. The fact that the I_a–V_a characteristic oscillates is a reflection of the existence of the spatially periodic nature of the electron transport properties within the gas. The oscillations have nothing to do with the properties of the grid per se, nevertheless the complex fields produced in the region of the latter are of some interest. The existence of such structures, and the 'window' of reduced field strengths E/n_0 in which the periodicity occurs, are on the other hand of considerable interest [55, 81], not in the least because this determines the conditions under which the experiment can actually operate as desired, to reflect quantization of the atoms.

The SST experiment is a deceptively simple example to treat theoretically, since there is no possibility of a reduced, hydrodynamic description through the diffusion equation [25]: although $(\partial f/\partial t) = 0$, the full Boltzmann equation (1) must be solved without any approximation of the spatial terms. The question of boundaries is a vexed one for charged particle kinetic theory, for even idealized problems, such as a perfectly absorbing boundary, are very difficult to handle, and approximations seem inevitable. As detailed in section 2.1.1, the Boltzmann equation requires only the values of f on the boundary for velocities directed *into* the region under investigation. For the truncated spherical harmonics representation (31), it is impossible to satisfy this sort of condition accurately, and one replaces it by certain conditions upon *one half* of the expansion coefficients, upon $f_m^{(l)}$ for either even or odd l. For the SST arrangement, for example, one specifies odd-l components at the source cathode, and even-l components at the anode [51]. For conservative collisions considered here the Legendre projections of the distribution function satisfy:

$$f_m^{(l)}(z_0, c) = f_{\mathrm{DM},m}^{(l)}(c) \qquad (l = 1, 3, \ldots, \text{ but } (l \neq 1, m \neq 0)), \tag{74}$$

$$f_m^{(l)}(z_0, c) = f_{s,m}^{(l)}(c) \qquad (l = 1, m = 0), \tag{75}$$

$$\frac{\partial}{\partial z} f_m^{(l)}(z_{\max}, c) = 0 \qquad (l = 0, 2, \ldots), \tag{76}$$

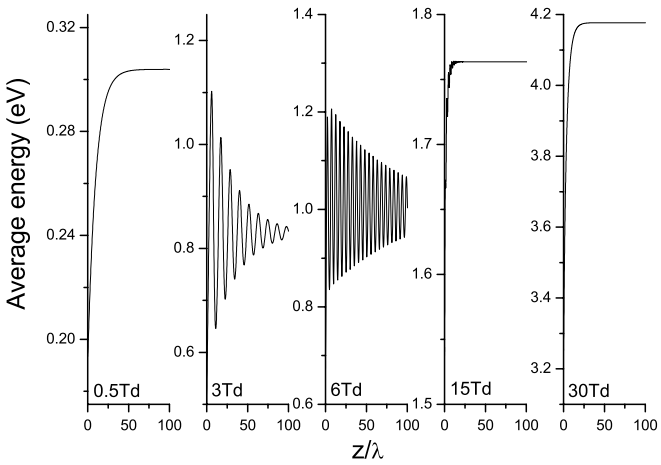

Figure 13. Spatial relaxation of the mean energy for the step function collision model (78) for various E/n_0 using a Boltzmann equation solution. Length is scaled according to $\lambda = \sqrt{2} n_0 \sigma_0$ where $\sigma_0 = 1\ \text{Å}^2$. The disturbing source is introduced via (77) with $T_i = 2.0 \times 10^3$ K and $v_i = 10^3\ \mathrm{m\,s^{-1}}$.

where $f_{s,m}^{(l)}(c)$ is the distribution under steady state hydrodynamic conditions. Thus effectively half the information about f is specified at each boundary. In (74), $f_{\mathrm{DM},m}^{(l)}(c)$ is the spherical harmonic component of the source distribution function, assumed to be a drifted Maxwellian,

$$f_{\mathrm{DM}}(\boldsymbol{c}) = A \left(\frac{m}{2\pi k T_i} \right)^{3/2} \exp\left[-\frac{m(\boldsymbol{c} - \boldsymbol{v}_i)^2}{2kT_i} \right], \tag{77}$$

with prescribed temperature and drift velocity parameters T_i and $\boldsymbol{v}_i$, respectively, and amplitude A. Condition (76) merely says that a constant value is reached at large distances from the source. For the fluid model, the choice concerns either even velocity moments (such as mean energy) or odd moments (such as mean velocity) at the respective boundaries.

To illustrate these considerations, we consider electrons in a model gas, using an inelastic step function model [54]:

$$\begin{aligned} &\sigma_m = 6\ \text{Å}^2, \\ &\sigma_i = 0.1\ \text{Å}^2, \qquad \varepsilon_i = 2\,\text{eV}, \\ &m_0 = 4\,\text{amu}, \qquad T_0 = 0\,\text{K}, \end{aligned} \tag{78}$$

where the inelastic collisions are characterized by a cross section σ_i and a threshold ε_i. Figure 13 displays the spatial evolution of average energy for a variety of E/n_0. The 'window' of electric field strengths for which the average energy (and other transport properties) exhibit oscillatory behaviour as they relax to the spatially uniform state is clearly in evidence, while the period of oscillation can be related to the threshold energy for the inelastic process and the field strength. The reader is referred to [36, 54, 81] for details.

Both the Franck–Hertz and SST experiments can also be analysed by a carefully formulated fluid model, particularly if a physical, semi-quantitative understanding is required as detailed below. The asymptotic profiles of the average energy using momentum transfer theory are displayed in figure 14 for the same system as considered in figure 13. We see that there is qualitative agreement in the structure of the profiles

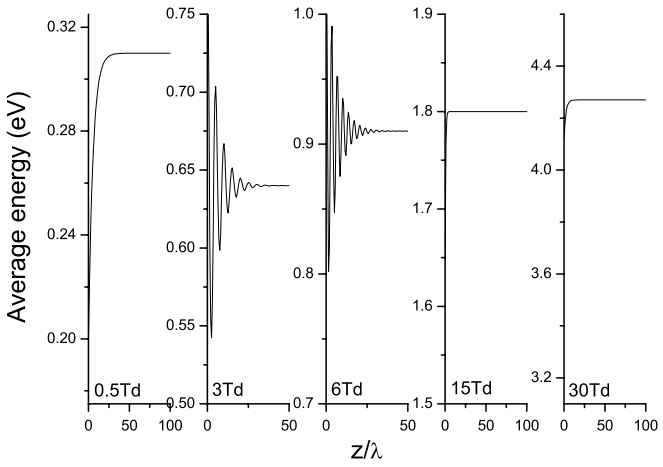

Figure 14. Spatial relaxation of the mean energy for the step function collision model (78) for various E/n_0 using momentum transfer theory. Conditions are as per figure 13.

and semi-quantitative agreement in both the window and the asymptotic periods of the oscillations within the window. The envelope for the damped periodic oscillations are, however, only qualitatively in agreement. Further details are given in [81].

An additional advantage of momentum transfer theory, however, is that it is particularly useful for explaining the window phenomenon in terms of the *ratio* of inelastic to elastic cross sections, through Ω as defined in equation (62), and the function

$$\eta = \frac{(1+\Omega')\,\varepsilon_\infty}{\varepsilon_\infty + \Omega - \frac{3}{2}kT_0}, \tag{79}$$

where ε_∞ is the asymptotic, spatially uniform mean energy. For values of E/n_0 such that η exceeds some critical value (see figure 3 of [81]), electronic properties are oscillatory, while outside this range, the same properties approach their asymptotic limits monotonically.

We are currently working on extending the non-hydrodynamic fluid treatment to include ions, parameterizing the heat flux term and benchmarking against a known analytic solution of Boltzmann's equation. This will facilitate a full fluid treatment of low-temperature plasmas using momentum transfer theory.

5. Conclusion

In this paper we have reviewed the application of Boltzmann and fluid equation methods to the transport of charged particles in low-temperature plasmas. In particular, we have focused on the unified treatment of electrons and ions, outlining a space and time-dependent multi-term solution of Boltzmann's equation valid for both electrons and ions. We have outlined the equivalent fluid equation treatment, proceeding directly from Boltzmann's equation and systematically outlining the necessary assumptions that must be made to close the system of equations and evaluate the collision terms involved. The momentum transfer approximation has been used to approximate collision terms in the fluid model, and the approximation has been benchmarked through comparison with Boltzmann equation solutions where possible. We have considered application of both Boltzmann equation and fluid equation treatments on problems of temporal and spatial non-locality, highlighting interesting and sometimes counter-intuitive behaviour in the associated transport properties, as well as focussing on the accuracy of commonly used approximations and assumptions.

Acknowledgments

All the authors would like to acknowledge the support of the Australian Research Council and the Centre for Antimatter-Matter Studies. This research is also funded in part by (i) Belgian Science Policy under contract IAP VI/11 and by IISN (PN), and (ii) the MNTRS project 141025 (SD).

References

[1] Becker K, Deutsch H and Inokuti M 2000 *Adv. At. Mol. Phys.* **43** 399
[2] Makabe T and Petrović Z Lj 2006 *Plasma Electronics: Applications to Microelectronic Device Fabrication* (New York: Taylor and Francis)
[3] Boltzmann L 1872 *Wein. Ber.* **66** 275
[4] Bogaerts A, Gijbels R and Goedheer W 1999 *Japan. J. Appl. Phys.* **38** 4404–15
[5] Vasenkov A V and Kushner M J 2003 *J. Appl. Phys.* **94** 5522–9
[6] Donko Z, Hartmann P and Kutasi K 2006 *Plasma Sources Sci. Technol.* **15** 178–86
[7] Tsendin L D 2009 *Plasma Sources Sci. Technol.* **18** 014020
[8] Huxley L G H and Crompton R W 1974 *The Drift and Diffusion of Electrons in Gases* (New York: Wiley)
[9] Crompton R W 1994 *Adv. At. Mol. Opt. Phys.* **32** 97
[10] Petrović Z Lj, Šuvakov M, Nikitović Z, Dujko S, Šašić O, Jovanović J, Malović G and Stojanović V 2007 *Plasma Sources Sci. Technol.* **16** S1
[11] Petrović Z Lj, Raspopović Z M, Stojanović V D, Jovanović J V, Malović G, Makabe T and de Urquijo J 2007 *Appl. Surf. Sci.* **253** 6619
[12] Wannier G H 1953 *Bell Syst. Tech. J.* **32** 170
[13] Allis W P 1956 *Handbuch der Physik* vol XXI (Berlin: Springer)
[14] Waldmann L 1958 *Handbuch der Physik* vol XII (Berlin: Springer) pp 295–514
[15] Kumar K 1966 *Ann. Phys.* **37** 113
[16] Kumar K 1966 *J. Math. Phys.* **7** 671
[17] Kumar K 1967 *Aust. J. Phys.* **20** 205
[18] Viehland L A and Mason E A 1975 *Ann. Phys.* **91** 499
[19] Viehland L A and Mason E A 1975 *Ann. Phys.* **110** 287
[20] Lin S L, Robson R E and Mason E A 1979 *J. Chem. Phys.* **71** 3483
[21] Kumar K, Skullerud H R and Robson R E 1980 *Aust. J. Phys.* **33** 343
[22] Mason E A and McDaniel E W 1988 *Transport Properties of Ions in Gases* (New York: Wiley)
[23] Robson R E 2006 *Introductory Transport Theory for Charged Particles in Gases* (Singapore: World Scientific)
[24] White R D, Ness K F and Robson R E 2002 *Appl. Surf. Sci.* **192** 26–49
[25] Robson R E, White R D and Petrović Z Lj 2005 *Rev. Mod. Phys.* **77** 1303–20
[26] Robson R E, Nicoletopoulos P, Li B and White R D 2008 *Plasma Sources Sci. Technol.* **17** 024020
[27] Wang-Chang C S, Uhlenbeck G E and De Boer J 1964 *Studies in Statistical Mechanics* vol II, ed J De Boer and G E Uhlenbeck (New York: Wiley) p 241

[28] Bzenić S, Raspopović Z M, Sakadžić S and Petrović Z Lj 1999 *IEEE. Trans. Plasma Sci.* **27** 78
[29] Raspopović Z, Sakadžić S, Petrović Z Lj and Makabe T 2000 *J. Phys. D: Appl. Phys.* **33** 1298
[30] Petrović Z Lj, Raspopović Z M, Dujko S and Makabe T 2002 *Appl. Surf. Sci.* **192** 1–21
[31] Dujko S, White R D, Ness K F, Petrović Z Lj and Robson R E 2006 *J. Phys. D: Appl. Phys.* **39** 4788
[32] Ness K F 1994 *J. Phys. D: Appl. Phys.* **27** 1848
[33] White R D, Ness K F, Robson R E and Li B 1999 *Phys. Rev.* E **60** 2231
[34] White R D, Robson R E and Ness K F 1999 *Phys. Rev.* E **60** 7457
[35] Li B, White R D, Robson R E and Ness K F 2001 *Ann. Phys.* **292** 179–98
[36] Li B, Robson R E and White R D 2006 *Phys. Rev.* E **74** 026405
[37] Loffhagen D and Winkler R 1996a *J. Phys. D: Appl. Phys.* **29** 618
[38] Winkler R 2000 *Adv. At. Mol. Opt. Phys.* **43** 19
[39] Winkler R, Loffhagen D and Sigeneger F 2002 *Appl. Surf. Sci.* **192** 50–71
[40] Maeda K, Makabe T, Nakano N, Bzenić S and Petrović Z Lj 1997 *Phys. Rev.* E **55** 5901
[41] Shimada T, Nakamura Y, Petrović Lj Z and Makabe T 2003 *J. Phys. D: Appl. Phys.* **36** 1936–46
[42] Trunec D, Bonaventura Z and Necas D 2006 *J. Phys. D: Appl. Phys.* **39** 2544–52
[43] Viehland L A 1994 *Chem. Phys.* **179** 71
[44] Montgomery D C and Tidman D A 1964 *Plasma Kinetic Theory* (New York: McGraw-Hill)
[45] Dyatko N A and Napartovich A P 2003 *J. Phys. D: Appl. Phys.* **36** 2096–101
[46] Loffhagen D 2005 *Plasma Chem. Plasma Process.* **25** 519–38
[47] Holt E H and Haskell R E 1965 *Plasma Kinetic Theory* (New York: MacMillan)
[48] Case K M and Zweifel P F 1967 *Linear Transport Theory* (Reading, MA: Addison-Wesley)
[49] Marshak R E 1947 *Phys. Rev.* **71** 443
[50] Mark C 1957 The spherical harmonics method I and II *Technical Report* CRT 338 and CRT 340, Atomic Energy of Canada Ltd
[51] Li B, White R D and Robson R E 2002 *J. Phys. D: Appl. Phys.* **35** 2914
[52] Porokhova I A, Yu B, Golubovskii B, Bretagne J, Tichy M and Behnke J F 2005 *Phys. Rev.* E **71** 066406
[53] Porokhova I A, Yu B, Golubovskii B, Bretagne J, Tichy M and Behnke J F 2005 *Phys. Rev.* E **71** 066407
[54] Robson R E, Li B and White R D 2000 *J. Phys. B: At. Mol. Opt. Phys.* **33** 507–20
[55] Sigeneger F, Winkler R and Robson R E 2003 *Contrib. Plasma Phys.* **43** 178–97
[56] Ness K F and Robson R E 1986 *Phys. Rev.* A **34** 2185
[57] Chapman S and Cowling T G 1939 *The Mathematical Theory of Non-uniform Gases* (Cambridge: Cambridge University Press)
[58] Brush S G 1972 *Kinetic theory* vol 3 (New York: Pergamon)
[59] Kihara T 1953 *Rev. Mod. Phys.* **25** 844
[60] Raspopović Z M, Sakadžić S, Bzenić S A and Petrović Z Lj 1999 *IEEE Plasma Sci.* **27** 1241
[61] Dyatko N A, Napartovich A P, Sakadžić S, Petrović Z Lj and Raspopović Z 2000 *J. Phys. D: Appl. Phys.* **33** 375–80
[62] Dujko S, Raspopović Z M, Petrović Z Lj and Makabe T 2003 *IEEE Trans. Plasma Sci.* **31** 711–6
[63] Suvakov M, Petrovic Z L, Marler J P, Buckman S J, Robson R E and Malovic G 2008 *New J. Phys.* **10** 053034
[64] Robson R E and Ness K F 1986 *Phys. Rev.* A **33** 2068
[65] Sakai Y, Tagashira H and Sakamoto S 1977 *J. Phys. D: Appl. Phys.* **10** 1035
[66] Tagashira H, Sakai Y and Sakamoto S 1977 *J. Phys. D: Appl. Phys.* **10** 1051
[67] White R D, Robson R E, Schmidt B and Morrison M A 2002 *J. Phys. D: Appl. Phys.* **35** 3125–31
[68] Ness K F and Robson R E 1985 *Transport Theory Stat. Phys.* **14** 257
[69] Ness K F 1985 *PhD Thesis* James Cook University
[70] Frost L S and Phelps A V 1962 *Phys. Rev.* **127** 1621
[71] Robson R E 1986 *J. Chem. Phys.* **85** 4486
[72] Vrhovac S B and Petrović Z Lj 1996 *Phys. Rev.* E **53** 4012
[73] Viehland L A and Goeringer D E 2005 *J. Phys. B: At. Mol. Opt. Phys.* **38** 3987
[74] Viehland L A, Kabbe E A and Dixit V V 2005 *J. Phys. B: At. Mol. Opt. Phys.* **38** 4011
[75] Goeringer D E and Viehland L A 2005 *J. Phys. B: At. Mol. Opt. Phys.* **38** 4027
[76] Robson R E 1984 *Aust. J. Phys.* **37** 35
[77] Tonks L 1937 *Phys. Rev.* **51** 744
[78] Heylen A E D 1980 *IEE Proc.* **127** 221
[79] Margeneau H 1946 *Phys. Rev.* **69** 508
[80] Petrović Z Lj and Vrhovac S B 1998 *Electron Kinetics and Application to Glow Discharges* vol 367, ed U Kortshagen and L D Tsendin (New York: Plenum) pp 441–58
[81] Nicoletopoulos P and Robson R E 2008 *Phys. Rev. Lett.* **100** 124502
[82] White R D, Dujko S, Ness K F, Robson R E, Raspopović Z M and Petrović Z Lj 2008 *J. Phys. D: Appl. Phys.* **41** 025206
[83] Loffhagen D and Winkler R 1999 *IEEE Plasma Sci. Technol.* **27** 1262
[84] White R D, Ness K F and Robson R E 1999 *J. Phys. D: Appl. Phys.* **32** 1842
[85] White R D 2001 *Phys. Rev.* E **64** 056409
[86] White R D, Robson R E and Ness K F 1995 *Aust. J. Phys.* **48** 925
[87] Skullerud H R 1969 *J. Phys. B: At. Mol. Phys.* **2** 696
[88] Robson R E, White R D and Makabe T 1997 *Ann. Phys.* **261** 74
[89] Boeuf J P and Pitchford L C 1995 *Phys. Rev.* E **51** 1376
[90] Makabe T, Nakano N and Yamaguchi Y 1992 *Phys. Rev.* A **45** 2520
[91] Nakano N, Shimura N, Petrović Z Lj and Makabe T 1994 *Phys. Rev.* E **49** 4455–65
[92] Hanne G F 1988 *Am. J. Phys.* **56** 696
[93] Bulos B R and Phelps A V 1976 *Phys. Rev.* A **14** 615